# Acid Rain Research

REPORT 19/1989

## Interpretation of Soil Data from the RAIN Project

Norwegian Institute for Water Research NIVA

# NIVA – REPORT

Norwegian Institute for Water Research NIVA


**Main Office**
P.O.Box 33, Blindern
N-0313 Oslo 3
Norway
Phone (47 2) 23 52 80
Telefax (47 2) 39 41 29

**Regional Office, Sørlandet**
Grooseveien 36
N-4890 Grimstad
Norway
Phone (47 41) 43 033
Telefax (47 41) 42 709

**Regional Office, Østlandet**
Rute 866
N-2312 Ottestad
Norway
Phone (47 65) 76 752

**Regional Office, Vestlandet**
Breiviken 5
N-5035 Bergen - Sandviken
Norway
Phone (47 5) 95 17 00
Telefax (47 5) 25 78 90



Report No.: 0-82073

Sub-No.:

Serial No.: 2294

Limited distribution:


Report Title:

Interpretation of Soil Data from the RAIN Project.


Date: November 1989

0-82073



Author (s):

J.O. Reuss



Topic group: Acid precipitation

Geographical area: Norway

Number of pages (incl. app.)

Contractor: MD, NTNF, Environment Canada, Environment Ontario, SNV (Sverige), CEGB (UK)

Contractors ref. (or NTNF-No) NTNF-No.: FK03



Abstract:

Process-oriented models for prediction of soil and water acidification at the catchment scale require soil chemical and physical data as input parameters. Choice of soil properties characteristic for an entire catchment poses a major dilemma. This report deals with the interpretation of analyses from about 200 soil samples collected 1983-86 from the 7 catchments included in the RAIN project (Reversing Acidification In Norway). Various statistical techniques are used to derive characteristic values for key soil parameters such as cation exchange capacity, base saturation, bulk density, and anion absorption.



4 keywords, Norwegian
1. sur nedbør
2. jordkjemi
3. reversibilitet
4. nedbørfelt

4 keywords, English
1. acid precipitation
2. soil chemistry
3. reversibility
4. catchment


Project leader

Richard F. Wright

For the Administration

Bjørn Olav Rosseland


ISBN 82-577-1596-4

# INTERPRETATION OF SOIL DATA FROM THE RAIN PROJECT

J.O. Reuss

Department of Agronomy
Colorado State University
Fort Collins, CO 80523
USA

30 October 1989

## INTRODUCTION

Process-oriented models for prediction of soil and water acidification at the catchment scale require soil chemical and physical data as input parameters. Such data are generally derived from soil analyses. Because of the natural heterogeneity of soil within catchments, the choice of values for soil properties characteristic for an entire catchment poses a major dilemma. Nevertheless such characteristic values must be specified to apply predictive models.

This report deals with the interpretation of soil analyses for the 7 catchments included in the RAIN project (Reversing Acidification In Norway) (Wright et al. 1988). These interpretations generally focus on the derivation of characteristic values for those soil parameters required for modelling purposes, particularly those required by MAGIC (Model for Acidification of Groundwater In Catchments) (Cosby et al. 1985). However, in some cases material of more general interest has been included.

Samples were collected and analyzed under the supervision of Dr. Erik Lotse of the Swedish Agricultural University at Uppsala. Methods of collection and analyses and data compilations are given by Lotse and Ottabong (1985) and Lotse (1989).

PART I reports interpretation of samples from the Sogndal site, while results from the Risdalsheia site are given in PART II. Anion adsorption results from both sites are reported separately in PART III.

**PART 1. SOGNDAL**

## 1. RELATIONSHIPS WITH CARBON CONTENT

### 1.1 Loss on Ignition versus Percent Carbon

A very close relationship (Figure 1.1) between loss on ignition and percent carbon is apparent. One outlier has been deleted from both the graphs and regressions involving carbon. This point was also inconsistent on the graph of CEC versus carbon, suggesting an error in the carbon determination. The regression equation is,

$$y = 2.97 + 1.97x \qquad r^2 = 0.950 \qquad n = 83 \qquad (2.1)$$

This close relationship suggests that the OM lost on ignition consistently contains about 1/1.97 or 51% carbon, slightly below the classical 58% but well within the range expected for surface soils (Jackson, 1958). The intercept seems a little high but it is probably affected by the scatter at the high points.

### 1.2 CEC(KCl) versus Percent Carbon

The relationship between neutral salt (KCl) pH and percent carbon is shown in Figure 1.2. The regression equation is,

$$y = -0.526 + .555x \qquad r^2 = 0.779 \qquad (2.2)$$

This not only indicates a close relationship, but perhaps more importantly shows that CEC is almost exclusively of organic origin. The scatter is mostly to the upper right of the graph suggesting that the errors may not be normally distributed about the linear regression line. However, there is probably little to be gained by using a log or log-log transform. The regression indicates a CEC at soil pH of about 0.56 meq/100 g soil for every 1% carbon, very much below the 4.9 meq/100 g suggested by Jackson (1958).

This suggests that at soil pH most of the CEC (nearly 90% if we accept the 4.9 figure) is not available due to protonation of the sites. The fact that virtually all charge is organic apparently is due to a minimum of soil development, at least as far as clay formation is concerned. In graph 2.2 the points are differentiated by depth, showing the generally lower CEC (due to lower carbon) in the deeper samples.

## 1.3 Base Saturation versus Percent Carbon

This relationship (Figure 1.3) is highly significant with an $r^2$ of 0.279 and 82 degrees of freedom. However, while the relationship may have a real component, a good part of it may be spurious. The high base saturation values fall at the low carbon values where CEC is low and thus analytical error is relatively high. There seems to be a differentiation between depths in the pattern. The implications of this have not been fully explored. The base saturation as calculated here includes $Ca^{2+}$, $Mg^{2+}$, $Na^{+}$, $K^{+}$ and $NH_4^{+}$. The MAGIC model does not use $NH_4^{+}$ and requires separate consideration of the other four cations.

## 1.4 pH versus Carbon

This relationship (Figure 1.4) is also highly significant. The linear regression equation is,

$$y = 5.35 - 0.0292x \quad r^2 = 0.366 \qquad (2.3)$$

Again the errors are not uniformly distributed. The pattern seems to reflect the lower base saturation at high carbon levels. These lower base saturation points in turn are associated with low pH. These high carbon and low pH points tend to be concentrated in the 0-15 cm depth. Thus the general pattern is one of greater acidity associated with high organic matter. It appears that as organic

matter accumulates there are insufficient bases to saturate the sites and the system becomes more acidic.

## 2.0 CATION EXCHANGE CAPACITY

In order to estimate either a single value of base saturation (BS) for the catchment or the site, or two values if broken out by depth, we must aggregate the CEC. At present no distinction is made among catchments. This assumes that there is no difference in cation exchange capacity among catchments. No such difference appears using ANOVA techniques on either the raw data or logarithmic or square root transformed data. Differences among depths are much greater than any differences among catchments.

Use of arithmetic means of CEC (meq/100 g) introduces a problem in that the effect of a few high values (where the variance is high) totally overshadows the effect of all lower values. Also the median values are well below the means, indicating skewness. Estimates of central tendencies were made using the raw data, as well as logarithmic and square root transformations (Table 2.1). The log transforms seem to over-correct a bit, i.e. while the distribution is much closer to normal than the raw data, the means tended to be somewhat lower than the medians, and chi square lack of fit test is still significant in two of the three cases. None of the lack of fits were significant for the square root transform so this estimate of central tendency, i.e. (mean of the square roots)$^2$, was selected.

As an example, normal probability plots for CEC of all samples for both the raw data and a square root transform are shown in Figure 2.1. The square root transform under corrects on the low end in this case, while there is a

tendency for the log transform (not shown) to over correct at the high end.

Aggregated values and estimates of CEC are as follows:

| | Aggregated CEC |
|---|---|
| All | 3.66 meq/100 g |
| 0-15 cm | 5.52 |
| >15 cm | 2.27 |

The P values in Table 2.1 are from a Chi square test using frequency histograms. This procedure was found to be highly sensitive to the number of divisions selected and was discontinued.

Another problem arises with this CEC data, in that the 1983 values are higher than those for 1984-1987, and this difference is highly significant. This is illustrated by the means plot for the square root transform (Figure 2.2). Estimates for the square root transform after dropping the 1983 data are also shown in Table 2.1.

## 3. BASE SATURATION

The MAGIC model tracks four base cations, i.e. $Ca^{2+}$, $Mg^{2+}$, $Na^{+}$, and K+. As these are handled individually in the model, the saturation, i.e. the fraction of the total charges occupied by the ion, are evaluated separately for each of these ions.

### 3.1 Ca Saturation

The Ca saturation was calculated individually for all samples, and the distributions examined using frequency histograms, and especially normal probability plots. Again, distributions were examined for logarithmic and square root transformations as well as the raw data. Means, medians, standard deviations, and estimates of central tendency were calculated in each case (Table 3.1). As used here, central tendency is the mean for the raw data, the geometric mean for the log transforms, and the

square of the mean of the transformed value for the square root transform. The total population of 91 samples used for this evaluation includes 44 from 0-15 cm, 41 from 15-30 cm and 5 from 15-45 cm. While many of the parameters varied substantially with depth, this was not the case for Ca saturation. However, for consistency with the other parameters results were calculated for all samples, for the 0-15 cm depth and, for samples from greater than 15 cm. Single value estimates for the catchments were taken from the total population.

Examples of normal probability plots and frequency histograms representing the 0-15 cm depth are shown in Figures 3.1 and 3.2. The untransformed data are obviously skewed toward the low end. Some skewness can be detected at the high end on the lognormal plots, while the skewness at the low end is not entirely eliminated when the square root transform is used. There is no clear preference between the transforms in the case illustrated, and this was often the case not only for the Ca saturation data, but also where the procedure was used for other parameters. The "N P Evaluation" column in Table 3.1 is a subjective evaluation from examination of the Normal Probability plots and was used as an aid in selecting the transformation used in the final summary. The lognormal distribution may be slightly superior to the square root for Ca saturation, but in the case of Mg saturation (Section 3.2), the square root transformation was better, and this was selected for use in the summary in both cases.

The use of a single value for Ca saturation derived from all observations over a four-year sampling period assumes that Ca saturation has not changed significantly over time and that any difference in Ca saturation due to treatment (acid addition) can safely be ignored. There is a significant year effect on Ca saturation (Figure 3.3), but it is due to low values in the first year. These low values apparently arise from the high CEC values observed in 1983

as noted in the previous section, as the extractable Ca values do not differ by years. Ca saturation values are determined from the square root transforms both with and without the 1983 data (Table 3.1). No significant difference was detected in Ca saturation between catchments or to a year-by-catchment interaction.

### 3.2 Mg Saturation

The Mg saturation values for the transformed and untransformed parameters are given in Table 3.2. In this case there are small but highly significant differences due to depth, with higher Mg saturation at 0-15 cm than in the deeper layers. Again, there are significant differences due to years (Figure 3.4), but the pattern is difficult to interpret, as the values observed in 1983 and 1984 are similar (approximately 0.044), with significantly lower values (0.029) in 1985 and intermediate values (0.036) in 1986. Interpretation is also made more difficult by the apparently higher CEC in 1983.

The extractable Mg values in 1983 are significantly higher than those for the later years (Figure 3.5). It is possible that this could represent some export from the treated catchments; however, there is no indication of an effect due to fields ($p = 0.24$), or a year-by-catchment interaction ($p = 0.79$).

The relationship of exchangeable Mg to Ca as shown in Figure 3.6 is also of interest. The slope of the zero intercept regression is 0.295 with an $r^2$ value of 0.65. This seems to be below the ratios of the output fluxes as reported by Wright et al. (1988), which range from 0.66 to 0.41, suggesting that the Mg is somewhat more mobile in the system than is Ca.

### 3.3 K Saturation

The depth effect is relatively minor for K saturation, so only one estimate was made for this parameter. Estimates

were arrived at in two ways, i.e. regression of exchangeable K on CEC, and estimates of central tendency from raw or transformed values of K saturation.

Where a close relationship exists, the saturation may be estimated by regressing the amount of the exchangeable ion on CEC. A plot of this relationship for K is shown in Figure 3.7. As can be seen from the figure, much of the variability arises from the 1983 values, so the regressions were calculated for the total data set and again without the 1983 values. The intercepts were found to be very nearly zero, so the final regression lines were calculated with zero intercept.

Regression parameters of interest include the following.

| | All data | Without 1983 |
|---|---|---|
| $r^2$ | 0.60 | 0.75 |
| Slope | 0.031 | 0.029 |
| s.e.(slope) | 0.0016 | 0.0013 |
| s.e.(est) | 0.092 | 0.052 |

While the fit is substantially improved by dropping the 1983 values, the slope, i.e. the estimate of K saturation is very nearly the same, indicating a K saturation value of about 0.03. The regression line shown is for the 1984-86 data only. This procedure has the disadvantage that it may be unduly influenced by a few high values; however, from the distribution of the points this does not seem to be a problem.

When the K saturation data were examined directly, it again became apparent that the 1983 data were highly variable, so these were dropped along with one other extreme outlier. The resulting normal probability plot for the square root transform is shown in Figure 3.8. The estimate of K saturation derived from the square root mean is 0.032, with a 95% confidence interval of 0.028 to 0.036. The

untransformed data were clearly skewed, however the mean of 0.034 was not greatly different. From the above considerations a value of 0.030 was arrived at as a general estimate of K saturation.

### 3.4 Na saturation

The values for Na saturation are very low, with a mean of 0.030 and a median of 0.017. Because of the low values the relative error is high. The difference between mean and medians again indicates substantial skewness, with the average heavily affected by a few high values. Also the 1983 samples were quite different from those in later years, as shown by the higher values and more scatter when Na is plotted against CEC (Figure 3.9). If Na is regressed against CEC the intercept is highly significant, and the slopes are higher when the regression is forced through zero rather than if an intercept is allowed (Table 3.3).

Slopes range from 0.007 to 0.018 depending on the assumptions. Furthermore, there is a tendency towards non-linearity when the anomalous 1983 data are dropped. Due to these difficulties regression methods were discarded for calculating Na saturation.

The skewness in the Na saturation data cannot be overcome by a square root transformation. On the basis of the Normal Probability plot the log-normal distribution was selected, so the population estimate is the geometric mean. The 1983 data had less effect on this estimate than on the regression estimates, the estimate for all observations is 0.024, and without 1983 the estimate is 0.022, with 95 percent confidence interval of about 20% of the estimate. Considering the uncertainties in the various methods this estimate was rounded to a value of 0.02.

## 4.0 DENSITY

### 4.1 Estimates of Density

The aggregation of density was handled in a very similar manner to the other parameters discussed above. The 1983 sampling was again anomalous, and was discarded. Apparently it was based on wet weights while the 1984-86 determinations were on dry weights. Again, distributions were highly skewed, and means, medians, and normal probability plots were examined before deciding on the most appropriate estimate. The lognormal distribution was again selected, and estimates represent the geometric means as shown in Table 4.1.

Estimates derived from untransformed means are about 10% higher than the geometric means, while square root transforms are intermediate.

## 4.2 Density Related Parameters

One interesting relationship is that between density and CEC. When density is regressed against CEC using a multiplicative model of the form,

$$Y = aX^b \qquad (5.1)$$

we obtain the regression relationship,

$$\text{Density} = 0.8101(\text{CEC})^{-.358}, \qquad (5.2)$$

with 67 observations and an $r^2$ of 0.82. This relationship is shown graphically in Figure 4.1. It apparently arises from the fact that both CEC and density are controlled almost entirely by the amount of organic matter.

Another interesting relationship is that between CEC by weight and CEC by volume. CEC by volume is a function of the measured CEC by weight and the density. Because CEC by weight is closely related to density, there is also a close relationship between CEC by volume and CEC by weight, as shown in Figure 4.2. This relationship is non-linear, and can be described by,

$$CEC(vol) = 8.125CEC(wt)^{-.6375}, \quad (5.3)$$

with an $r^2$ of 0.935. Even though density decreases with increasing CEC(wt) this is not sufficient to compensate for the higher cation exchange capacity of the high carbon-low density organic matter. Thus, CEC by volume increases with increasing CEC(wt).

## 5.0 SUMMARY

A summary table (5.1) has been prepared for the Sogndal catchments showing the best estimates of the aggregated values of the parameters required by the MAGIC model. While these may change with further analysis of these or later data, the modifications are likely to be relatively small.

Table 2.1. Sogndal. Estimates of central tendency for cation exchange capacity (meq/100 g). Lack of fit by chi square.

| Depth | Mean | Median | s.d. | Central Tendency | Lack of fit (P) |
|---|---|---|---|---|---|
| Raw Data: | | | | | |
| All | 4.599 | 3.43 | 4.19 | 4.60[1] | 0.000**** |
| 0-15 cm | 6.441 | 5.40 | 4.66 | 6.44 | 0.053* |
| >15 cm | 2.875 | 1.79 | 2.80 | 2.88 | 0.000**** |
| Log Transform (base 10) | | | | | |
| All | 0.436 | 0.54 | 0.50 | 2.73[2] | 0.066 |
| 0-15 | 0.617 | 0.73 | 0.20 | 4.44 | 0.189 |
| >15 | 0.238 | 0.25 | 0.46 | 1.73 | 0.17 |
| Square Root Transform | | | | | |
| All | 1.914 | 1.85 | 0.97 | 3.66[3] | 0.124 |
| 0-15 | 2.349 | 2.32 | 0.97 | 5.52 | 0.505 |
| >15 | 1.507 | 1.34 | 0.75 | 2.27 | 0.12 |
| Square Root Transform (Without 1983) | | | | | |
| All | 1.678 | 1.59 | 0.89 | 2.82[3] | na |
| 0-15 | 2.112 | 2.14 | 0.89 | 4.46 | na |
| >15 | 1.281 | 1.00 | 0.69 | 1.64 | na |

[1] Mean
[2] Geometric mean
[3] Square of square root mean

Table 3.1. Sogndal. Estimates of central tendency and associated parameters for Ca saturation. N P evaluation is a subjective evaluation of the normal probability plot. Categories are Very Good, Good, Fair, and Poor.

| Depth | Mean | Median | s.d. | Central Tendency | N P Evaluation |
|---|---|---|---|---|---|
| Raw Data: | | | | | |
| All | 0.193 | 0.155 | 0.155 | 0.193[1] | P |
| 0-15 cm | .197 | .169 | .169 | .169 | F |
| >15 cm | .190 | .145 | .147 | .190 | P |
| Log Transform (base e) | | | | | |
| All | -1.843 | -1.863 | .638 | .158[2] | G |
| 0-15 | -1.777 | -1.777 | .570 | .169 | F |
| >15 | -1.904 | -1.927 | .691 | .149 | G |
| Square Root Transform | | | | | |
| All | .418 | .394 | .135 | .175[3] | F |
| 0-15 | .428 | .412 | .119 | .183 | G |
| >15 | .410 | .381 | .149 | .168 | F |
| Square Root Transform (Without 1983) | | | | | |
| All | .448 | .409 | .135 | .201[3] | na |
| 0-15 | .456 | .444 | .115 | .208 | na |
| >15 | .440 | .389 | .151 | .194 | na |

[1] Mean
[2] Geometric mean
[3] Square of square root mean

Table 3.2. Sogndal. Estimates of central tendency and associated parameters for Mg saturation. N P evaluation is a subjective evaluation of the normal probability plot. Categories are Very Good, Good, Fair, and Poor.

| Depth | Mean | Median | s.d. | Central Tendency | N P Evaluation |
|---|---|---|---|---|---|
| Raw Data: | | | | | |
| All | .0423 | .038 | .021 | .042[1] | F |
| 0-15 cm | .051 | .047 | .021 | .051 | G |
| >15 cm | .033 | .030 | .018 | .033 | P |
| Log Transform (base e) | | | | | |
| All | -3.157 | -3.280 | .533 | .043[2] | G |
| 0-15 | -3.064 | -3.058 | .449 | .047 | F |
| >15 | -3.546 | -3.546 | .502 | .029 | G |
| Square Root Transform | | | | | |
| All | .197 | .194 | .051 | .039[3] | VG |
| 0-15 | .221 | .217 | .047 | .049 | G |
| >15 | .175 | .172 | .045 | .031 | G |
| Square Root Transform (without 1983) | | | | | |
| All | .193 | .187 | .050 | .037[3] | na |
| 0-15 | .217 | .215 | .044 | .047 | na |
| >15 | .171 | .171 | .046 | .0296 | na |

[1] Mean
[2] Geometric mean
[3] Square of square root mean

Table 3.3. Sogndal. Regression parameters for the regression of exchangeable Na on CEC.

| | With Intercept | | Without Intercept | |
|---|---|---|---|---|
| | All points | w/o 1983 | All points | w/o 1983 |
| $r^2$ | 0.443 | 0.707 | 0.406 | 0.333 |
| Constant | 0.026 | 0.026 | 0 | 0 |
| Slope | 0.015 | 0.007 | 0.018 | 0.011 |
| s.e.(slope) | 0.0017 | 0.0006 | 0.0012 | 0.0006 |
| s.e.(est) | 0.069 | 0.016 | 0.070 | 0.024 |

Table 4.1. Sogndal. Geometric means and confidence intervals for density.

| Depth | n | Estimated Density | Confidence Interval (95%) |
|---|---|---|---|
| All | 68 | 0.618 kg/l | 0.585-0.653 |
| 0-15 cm | 33 | 0.511 | 0.479-0.546 |
| >15 | 37 | 0.738 | 0.694-0.785 |

Table 5.1. Sogndal. Summary table of aggregated values of soil parameters for use in the MAGIC Model.

| Depth | Density | CEC | Base Saturation | | | |
|---|---|---|---|---|---|---|
| | | | Ca | Mg | K | Na |
| cm | kg/l | meq/100g | ------Equivalent Fraction------ | | | |
| All | 0.618 | 3.66 | 0.175 | 0.039 | 0.03 | 0.02 |
| 0-15 | 0.511 | 5.52 | 0.183 | 0.049 | 0.03 | 0.02 |
| > 15 | 0.738 | 2.25 | 0.168 | 0.031 | 0.03 | 0.02 |

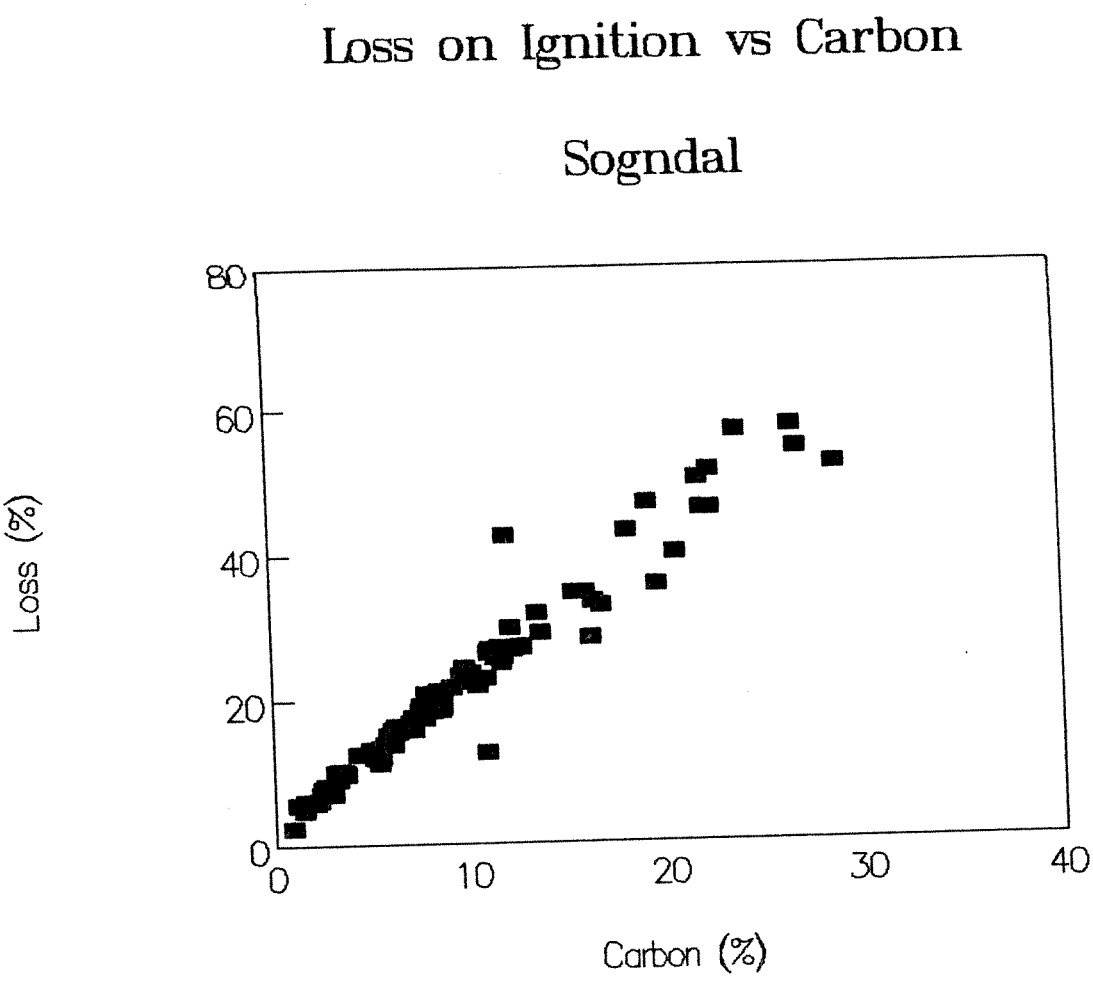


FIGURE 1.1. Sogndal. Loss on ignition as a function of percent carbon as determined by a chromic acid wet digestion.

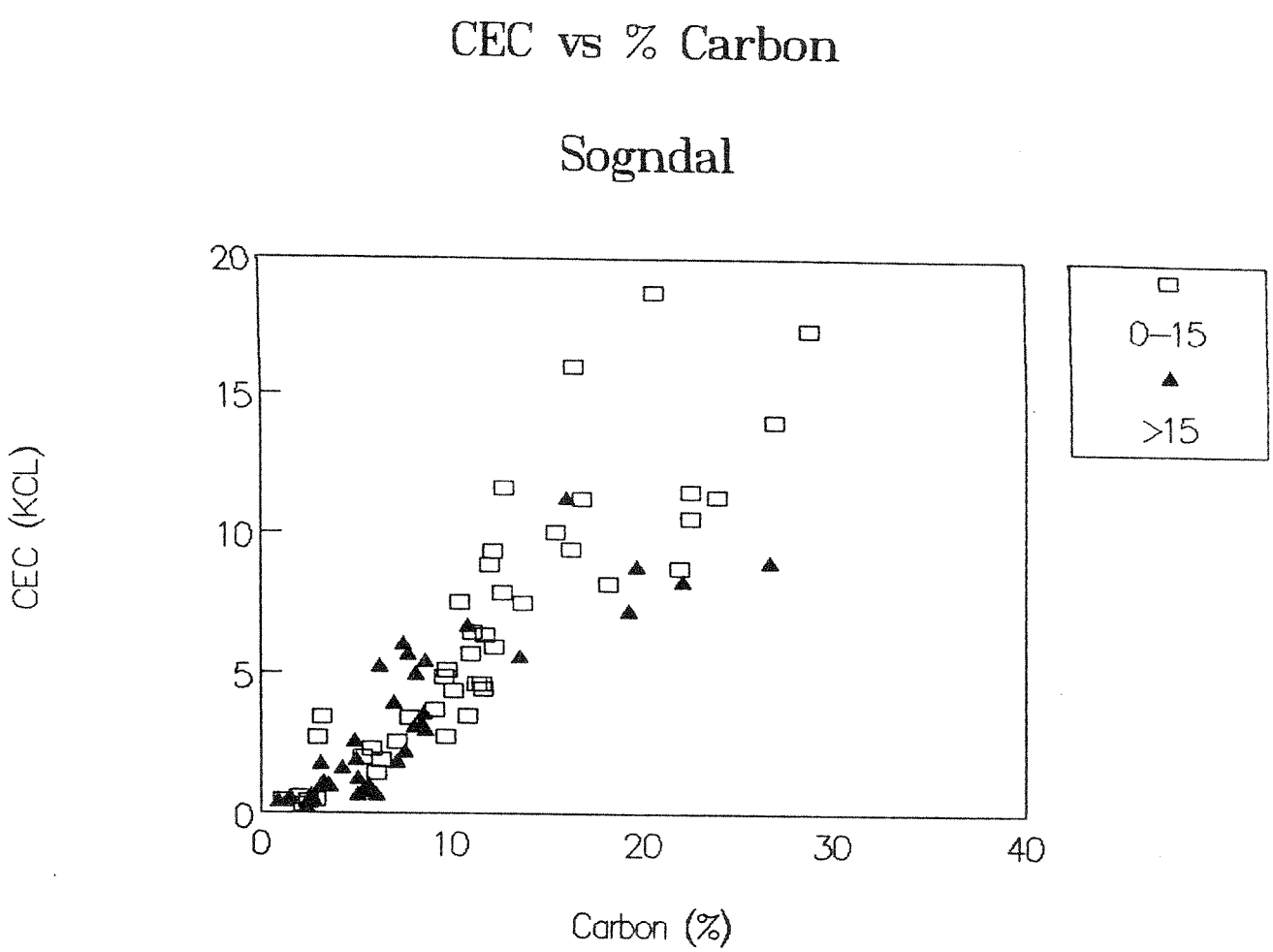


FIGURE 1.2. Sogndal. Cation exchange capacity (KCl) in meq/100g as function of percent carbon. Surface samples (0-15 cm) are shown by open boxes; deeper samples (>15 cm) are shown by triangles.

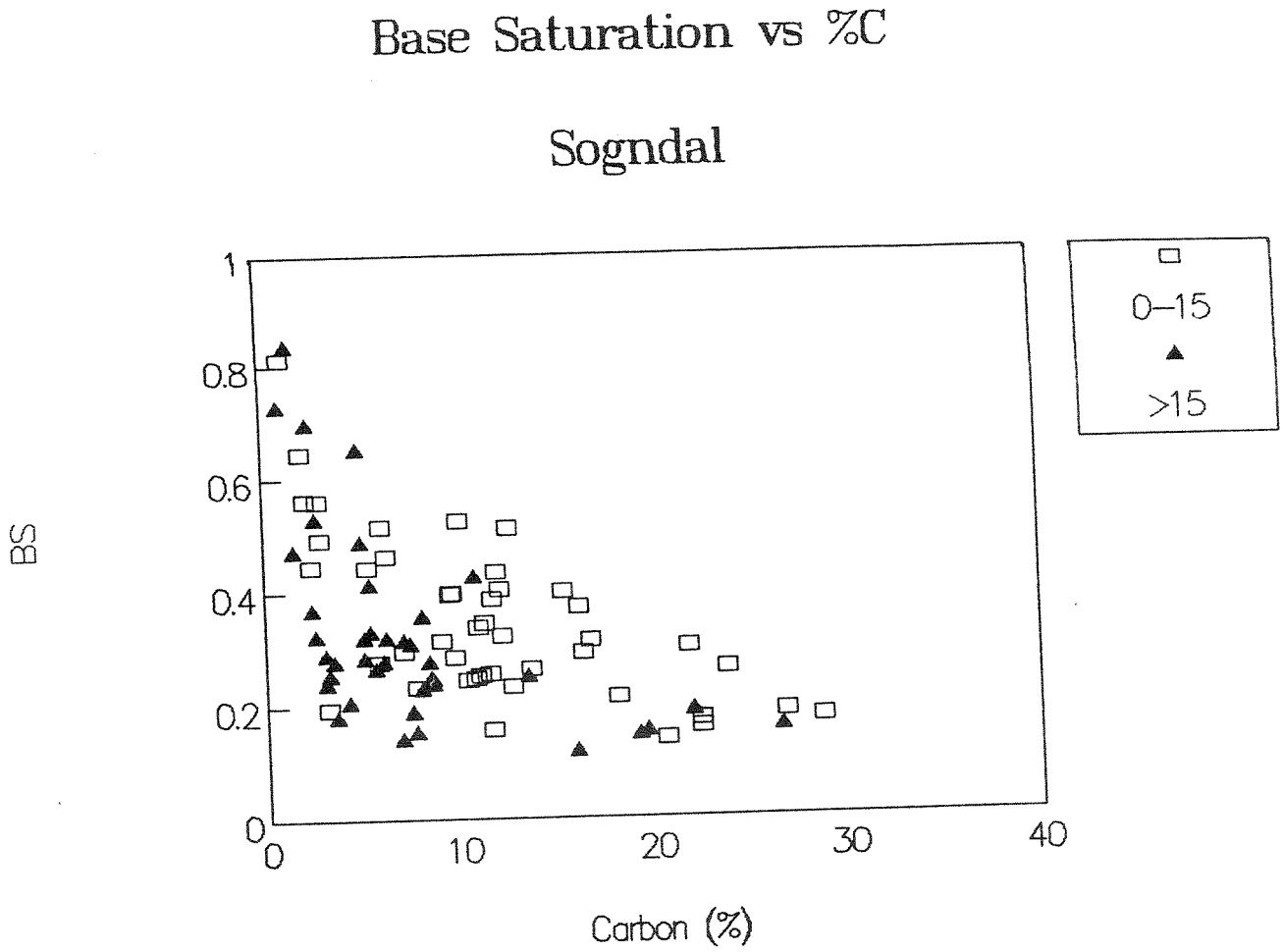


FIGURE 1.3. Sogndal. Base saturation as a function of percent carbon. Surface samples (0-15 cm) are shown by open boxes; deeper samples (>15 cm) are shown by triangles.

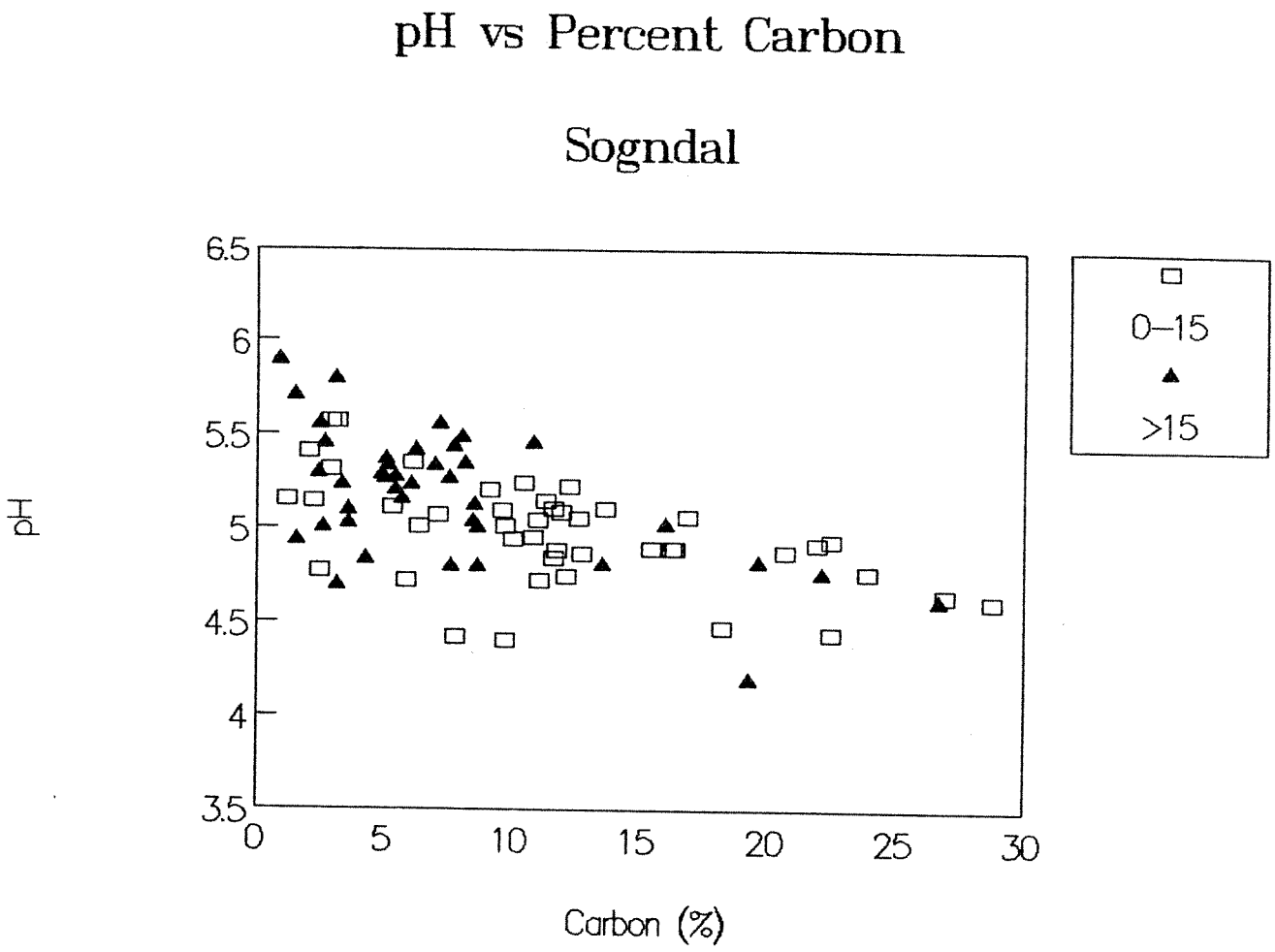


FIGURE 1.4. Sogndal. pH as a function of percent carbon. Surface samples (0-15 cm) are shown by open boxes; deeper samples (>15 cm) are shown by triangles.

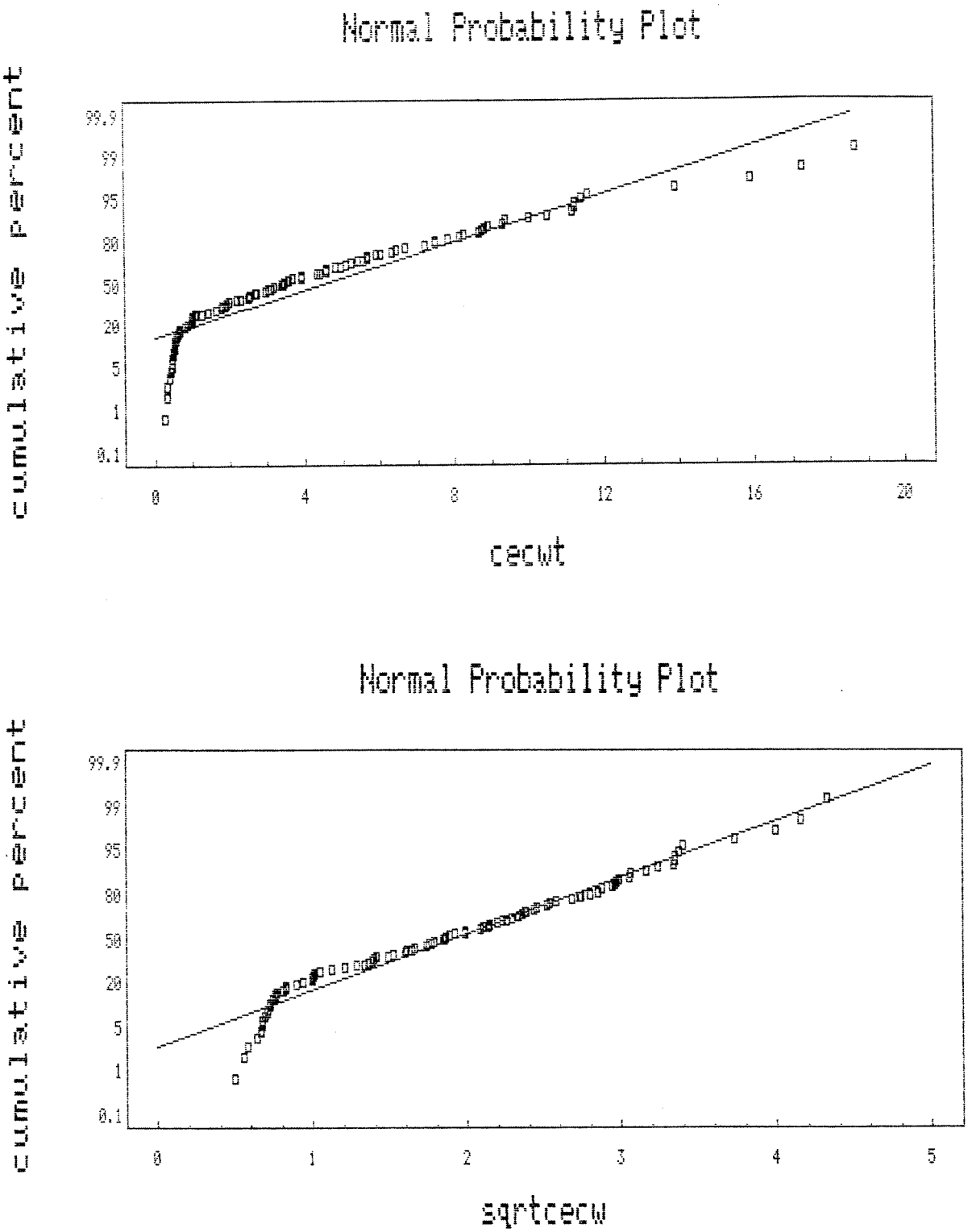


FIGURE 2.1. Sogndal. Normal probability plots for cation exchange capacity by weight, and for the square root transform of the same data.

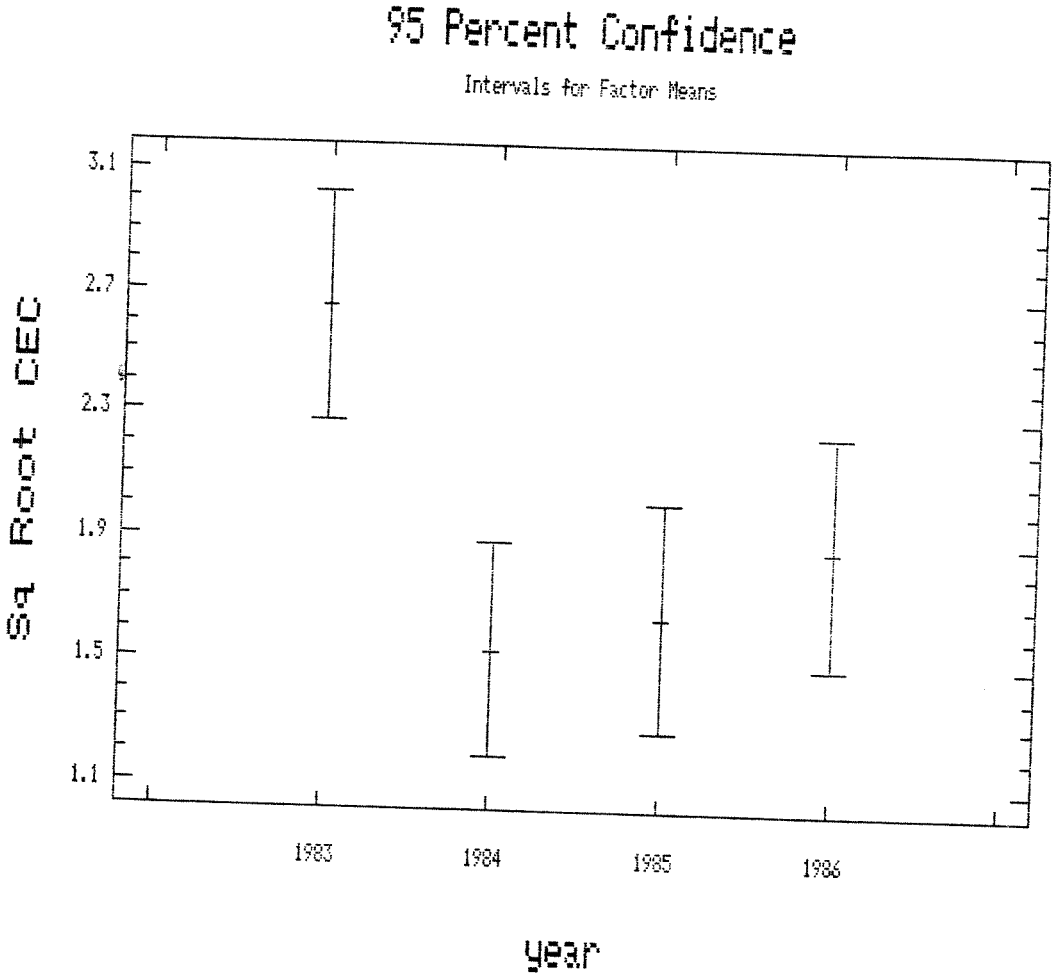


FIGURE 2.2. Sogndal. Means plot showing the 95% confidence interval for the square root transform of CEC by year.

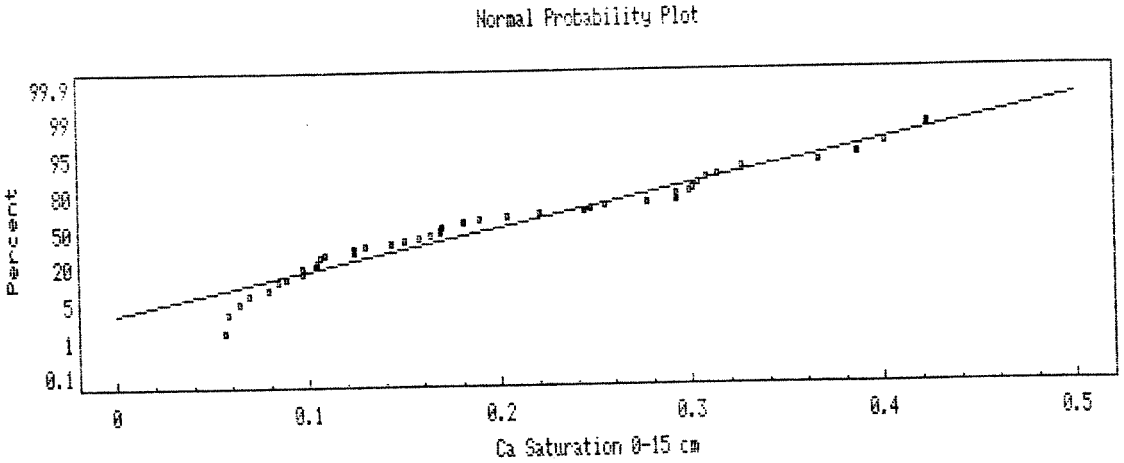


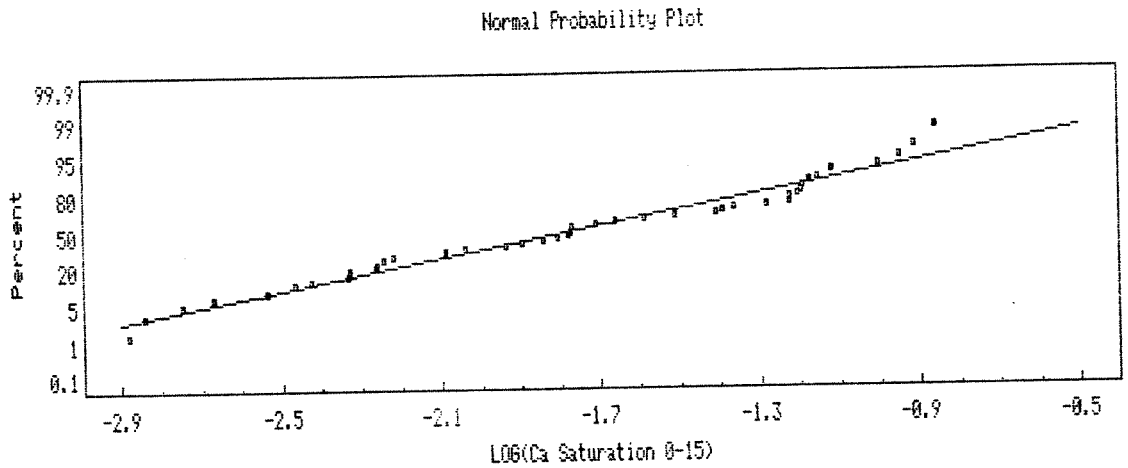


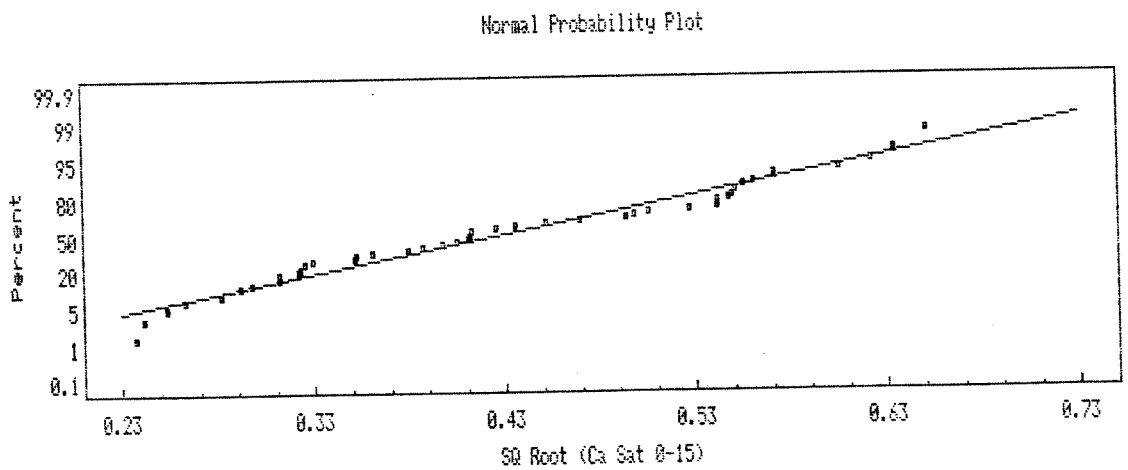


FIGURE 3.1. Sogndal. Normal Probability plots for the Ca saturation data from the 0-15 cm depth. Plots are shown for the raw data, log transform, and square root transform.

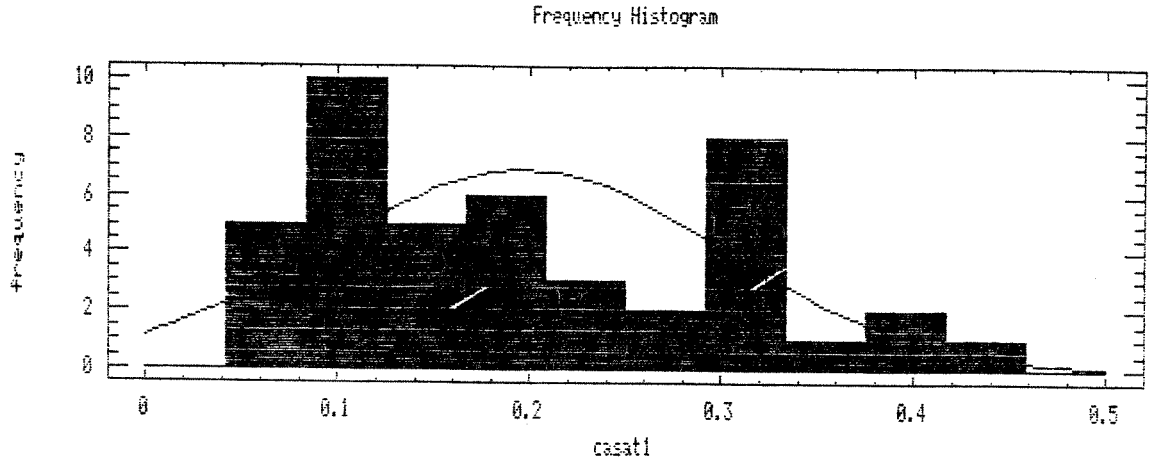


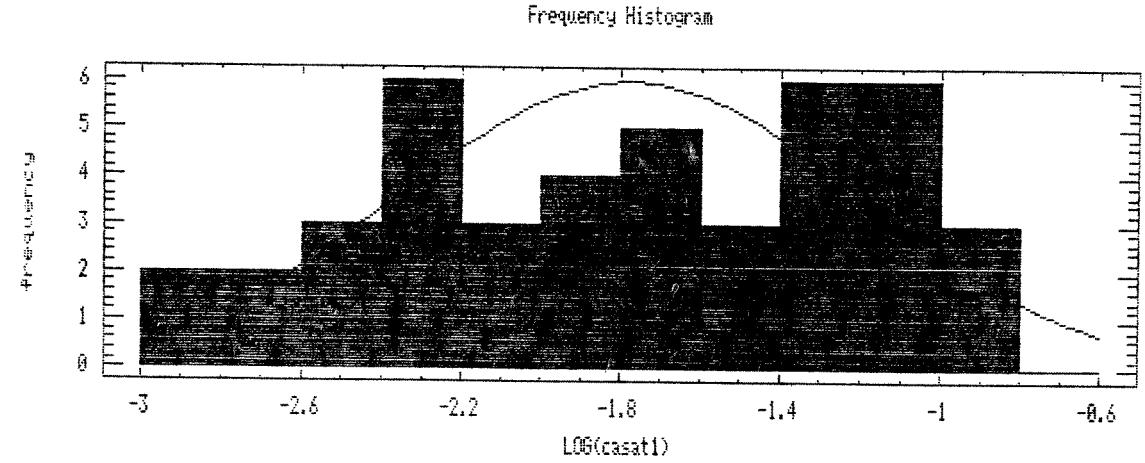


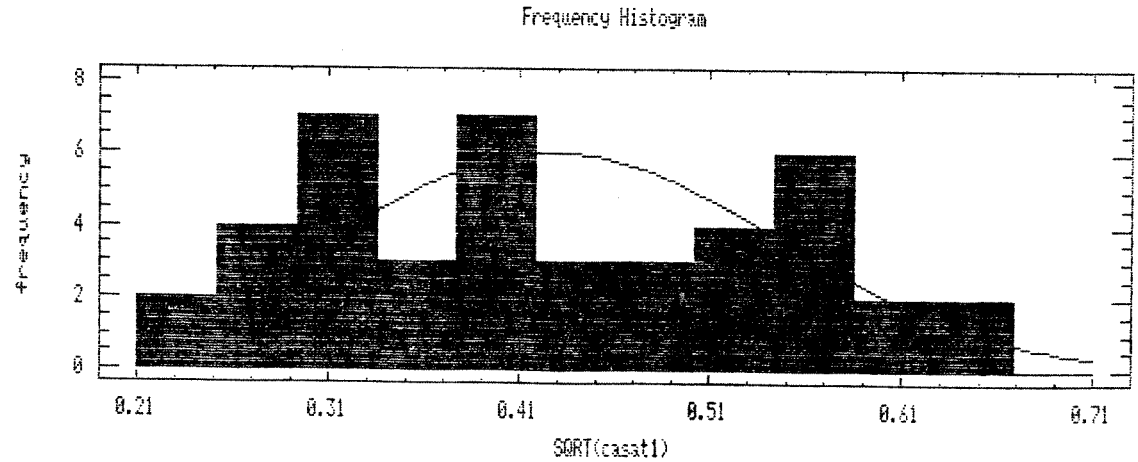


FIGURE 3.2. Sogndal. Frequency histograms for the Ca saturation data from the 0-15 cm depth. Histograms are shown for the raw data, log transform, and square root transform.

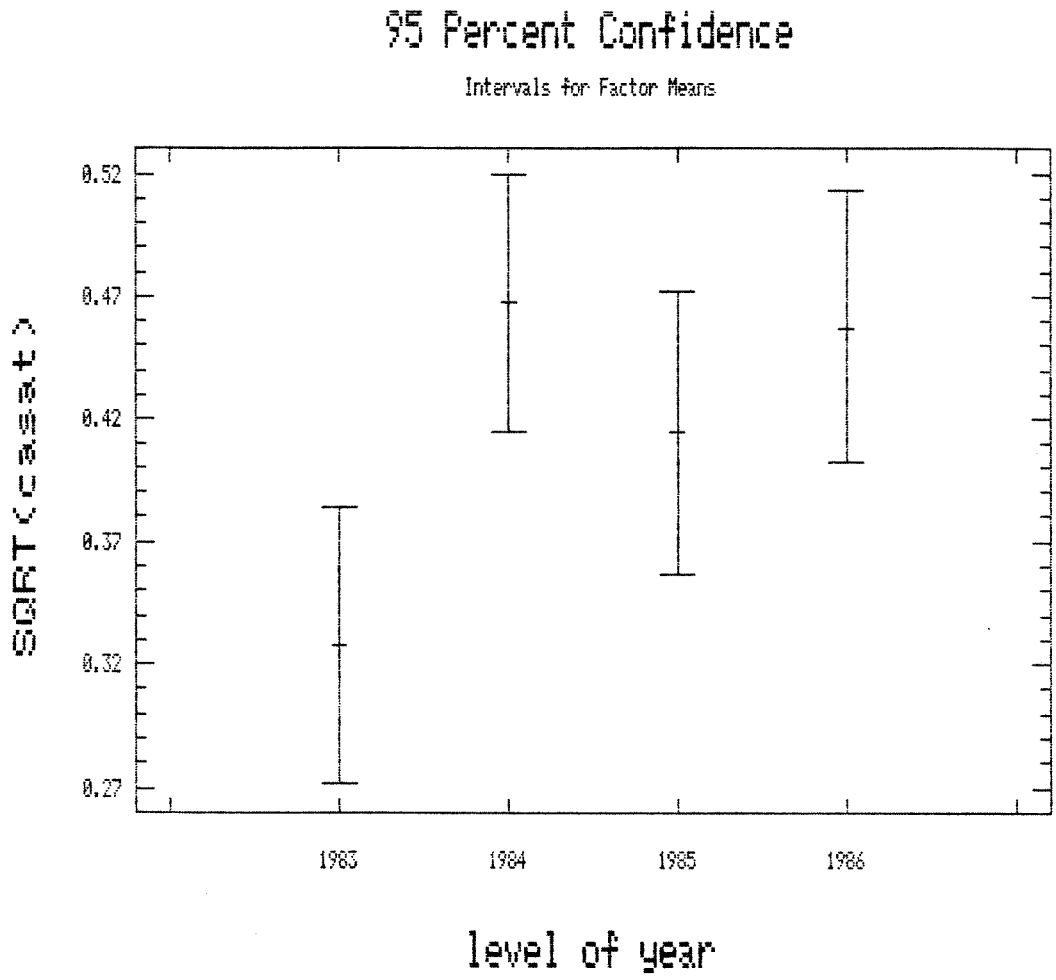


FIGURE 3.3. Sogndal. Means plot showing the 95% confidence interval for the square root transform of Ca saturation by year.

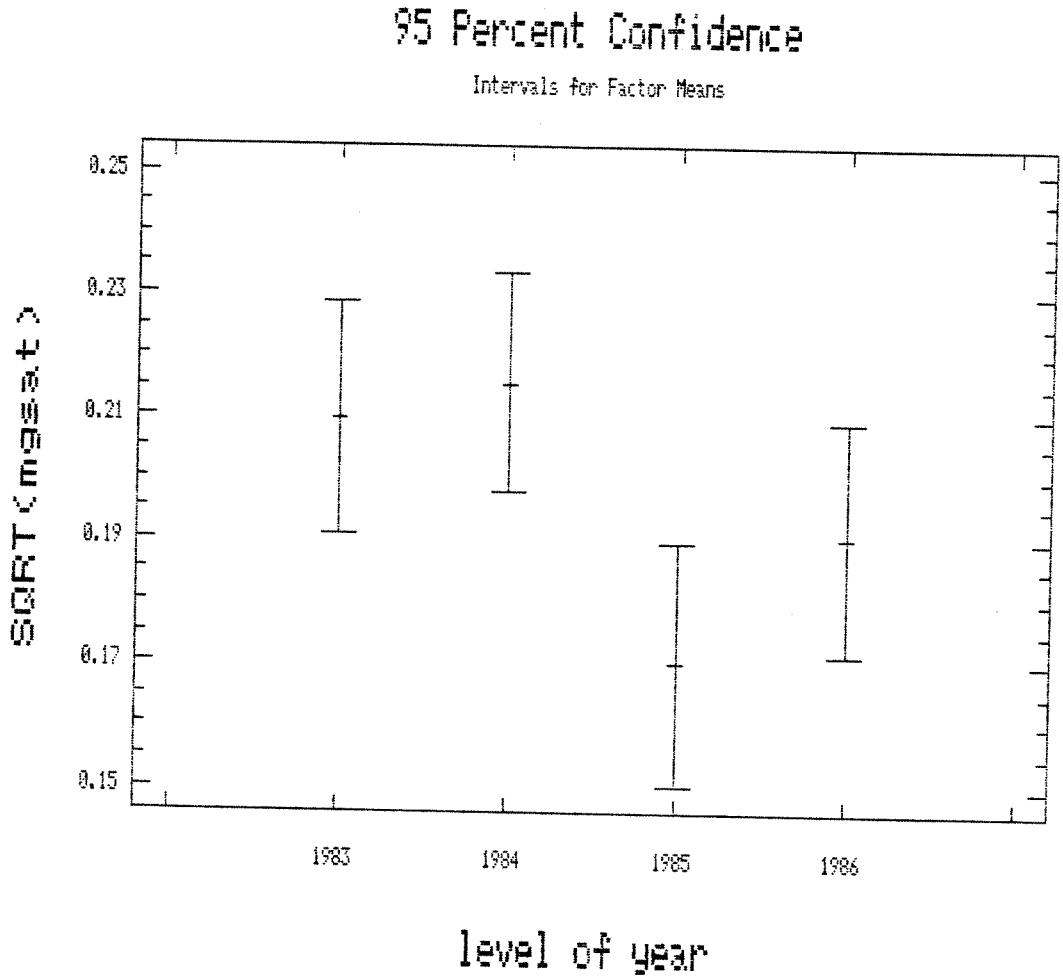


FIGURE 3.4. Sogndal. Means plot showing the 95% confidence interval for the square root transform of Mg saturation by year.

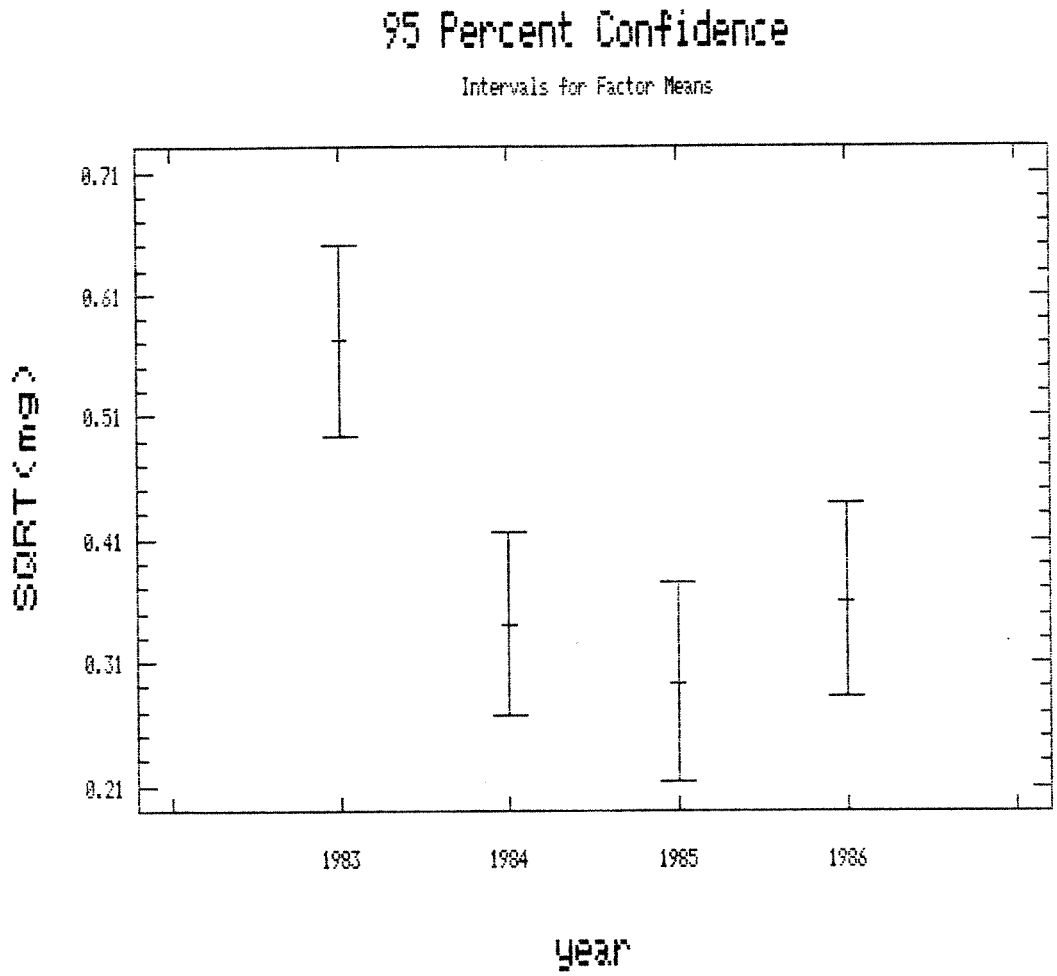


FIGURE 3.5. Sogndal. Means plot showing the 95% confidence interval for the square root transform of exchangeable Mg (meq/100g) by year.

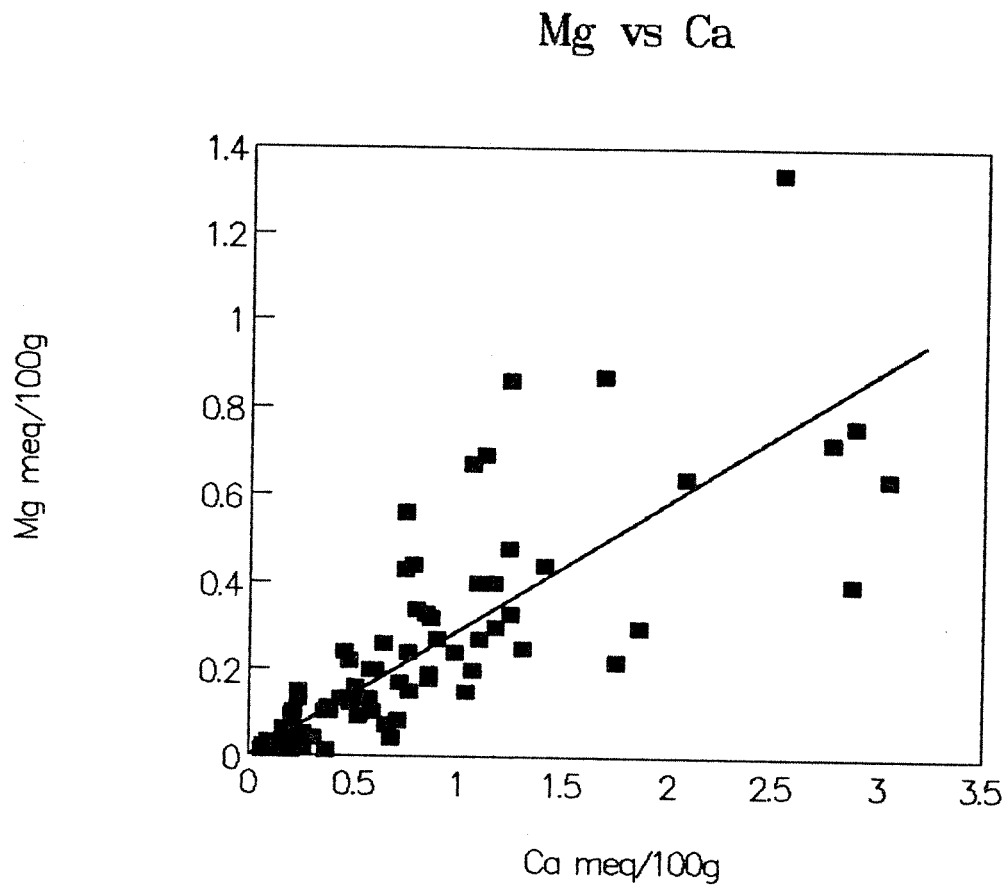


FIGURE 3.6. Sogndal. The relationship of exchangeable Mg and exchangeable Ca. The slope of the zero intercept regression equation is 0.295, with an $r^2$ of 0.65.

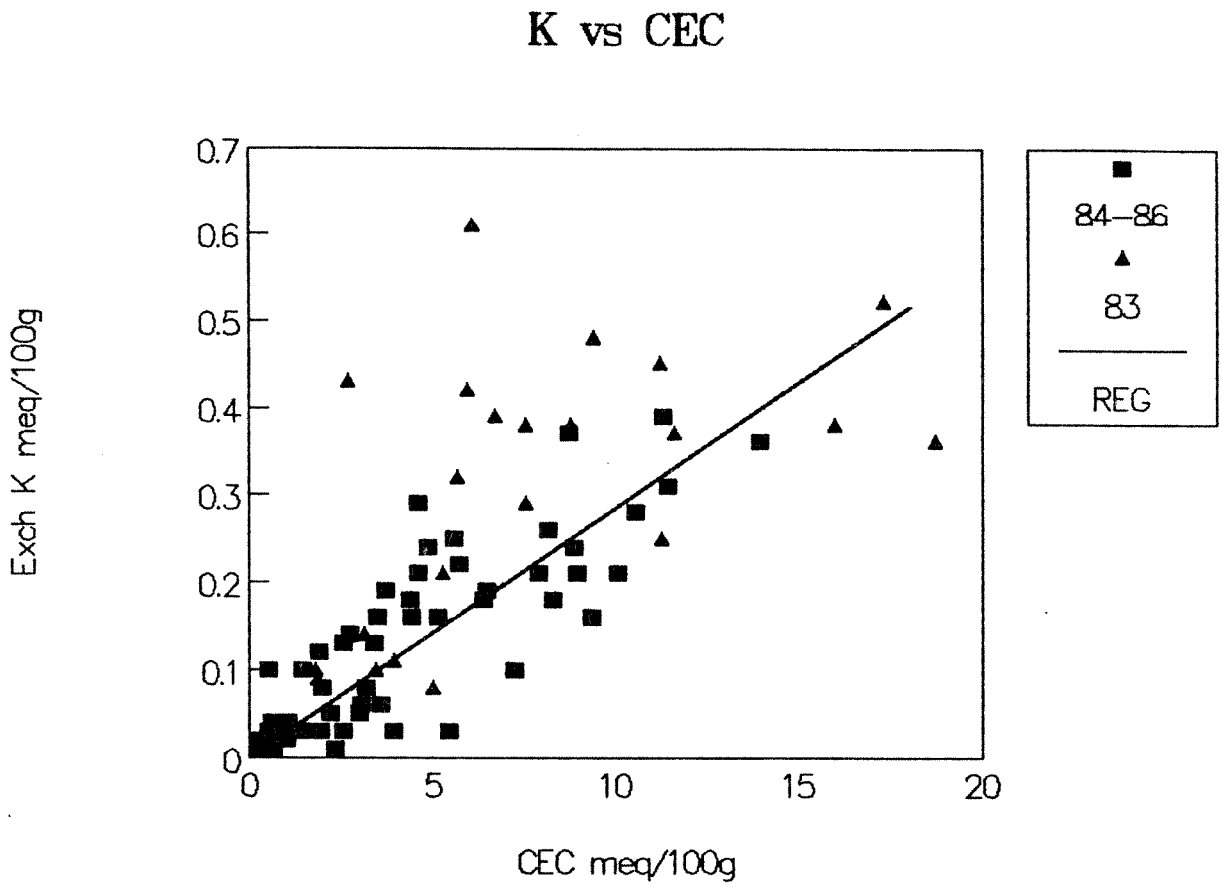


FIGURE 3.7. Sogndal. The relationship between exchangeable K and CEC, with the 1983 points differentiated. The slope of the zero intercept regression (without 1983) is 0.029 with an $r^2$ of 0.75.

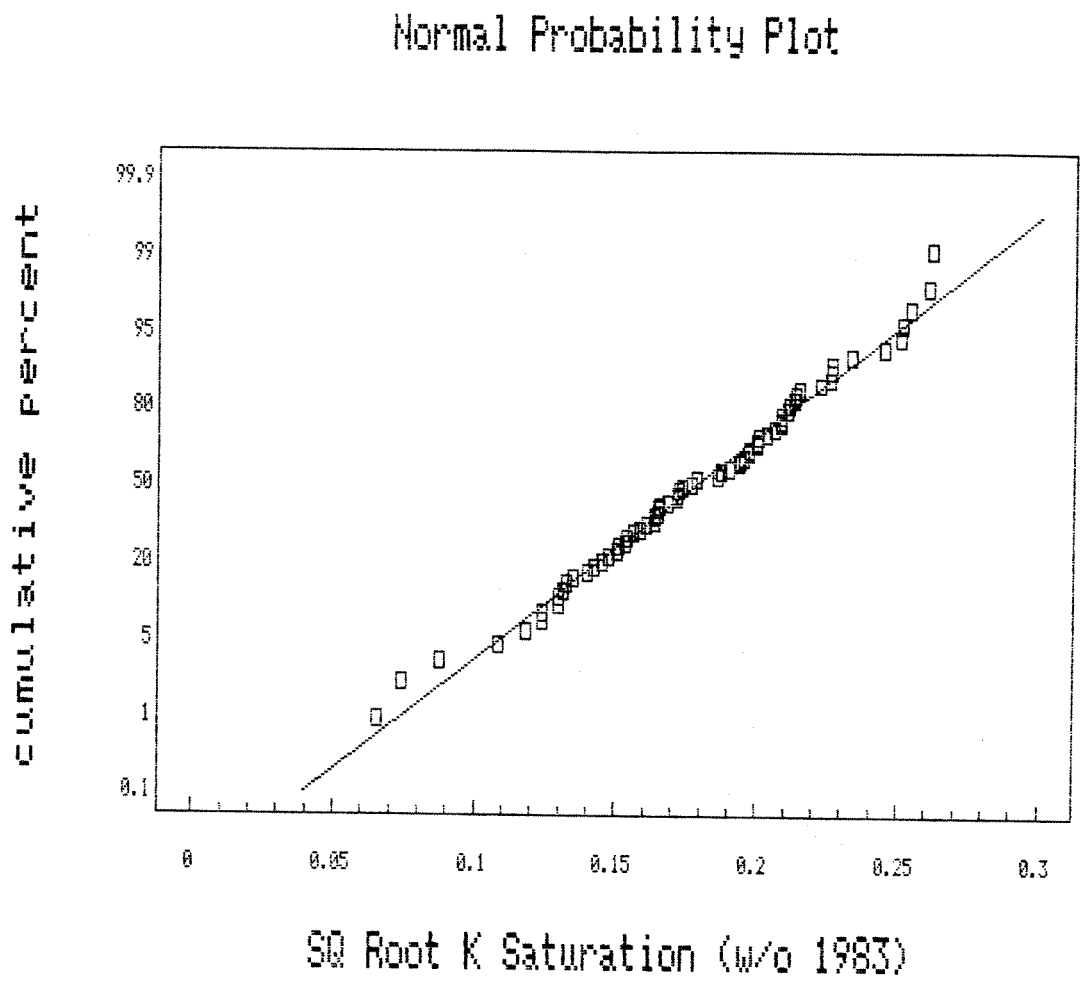


FIGURE 3.8. Sogndal. Normal probability plot for the square root transformed K saturation data.

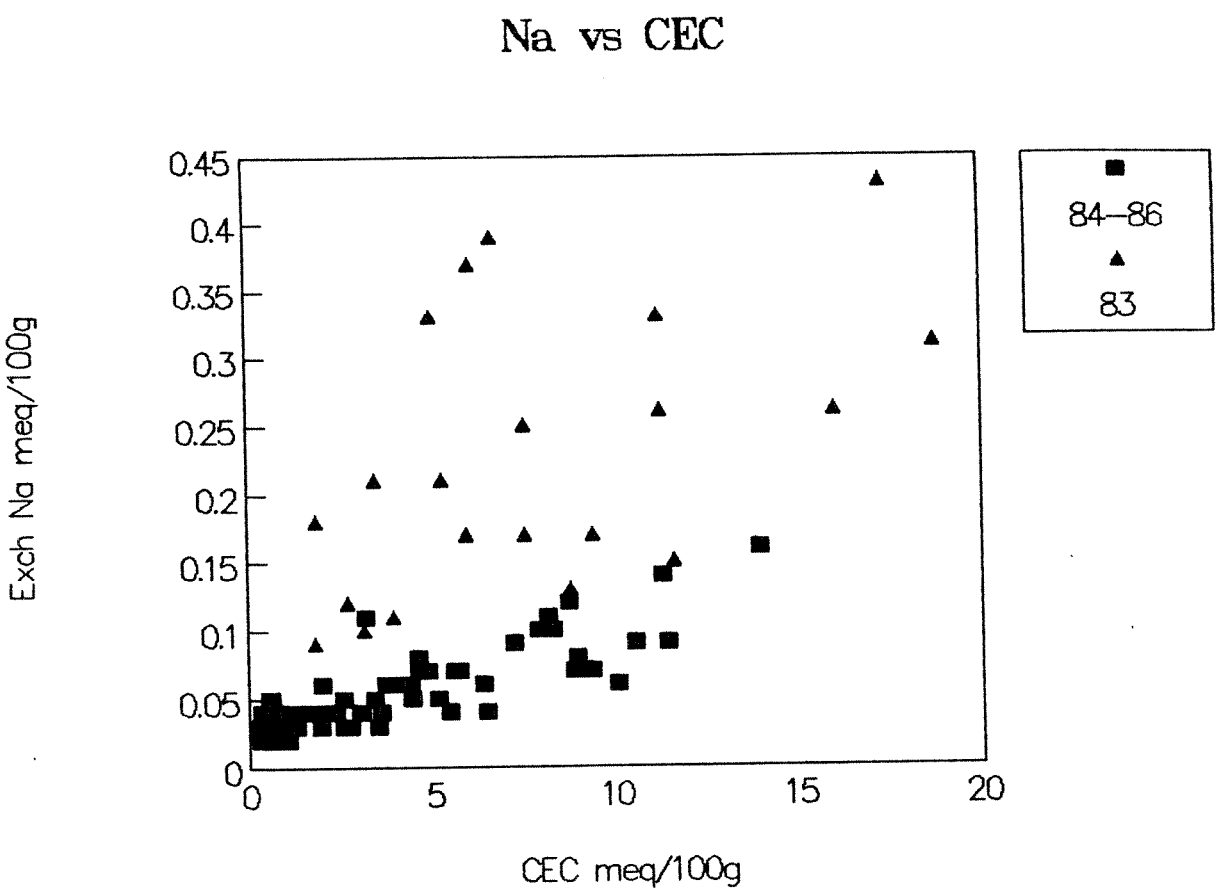


FIGURE 3.9. Sogndal. Plot of exchangeable Na as a function of CEC with the 1983 data differentiated.

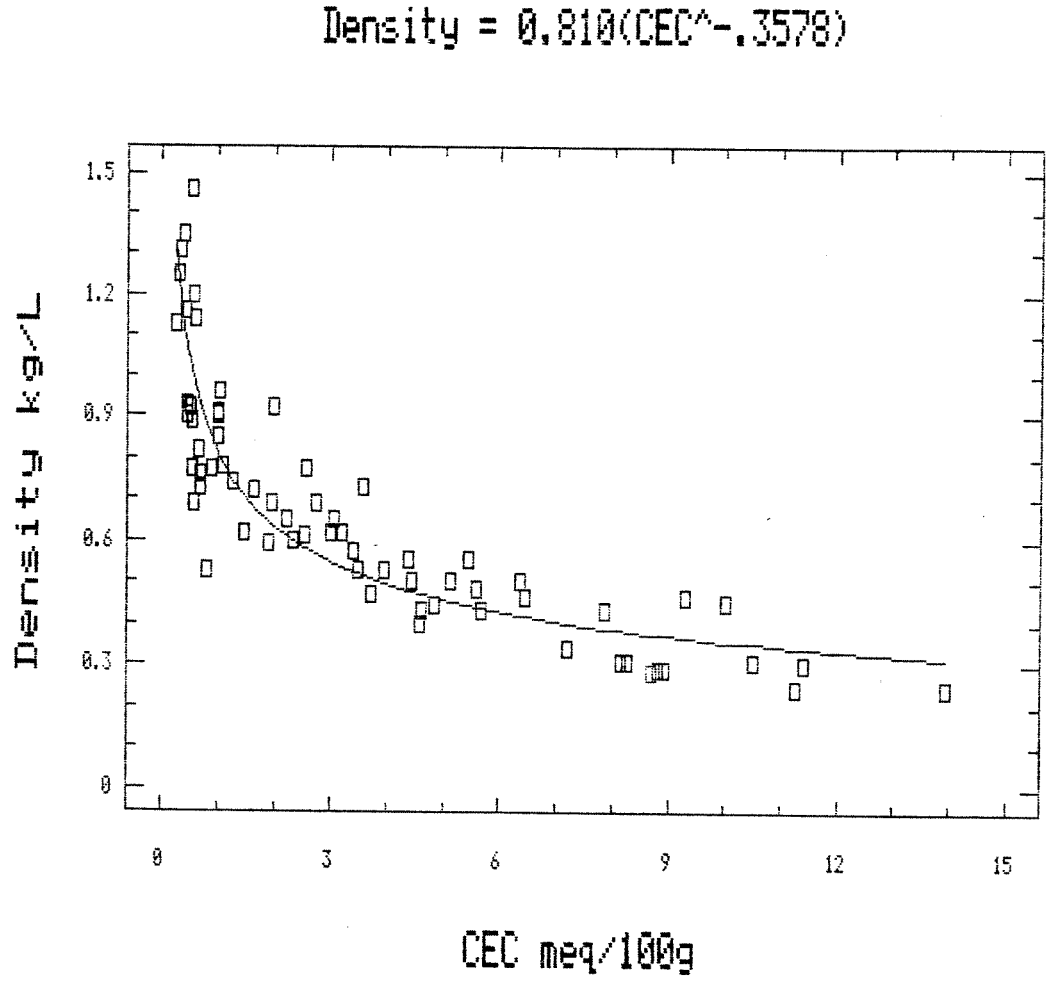


FIGURE 4.1. Sogndal. The relationship between density and cation exchange capacity.

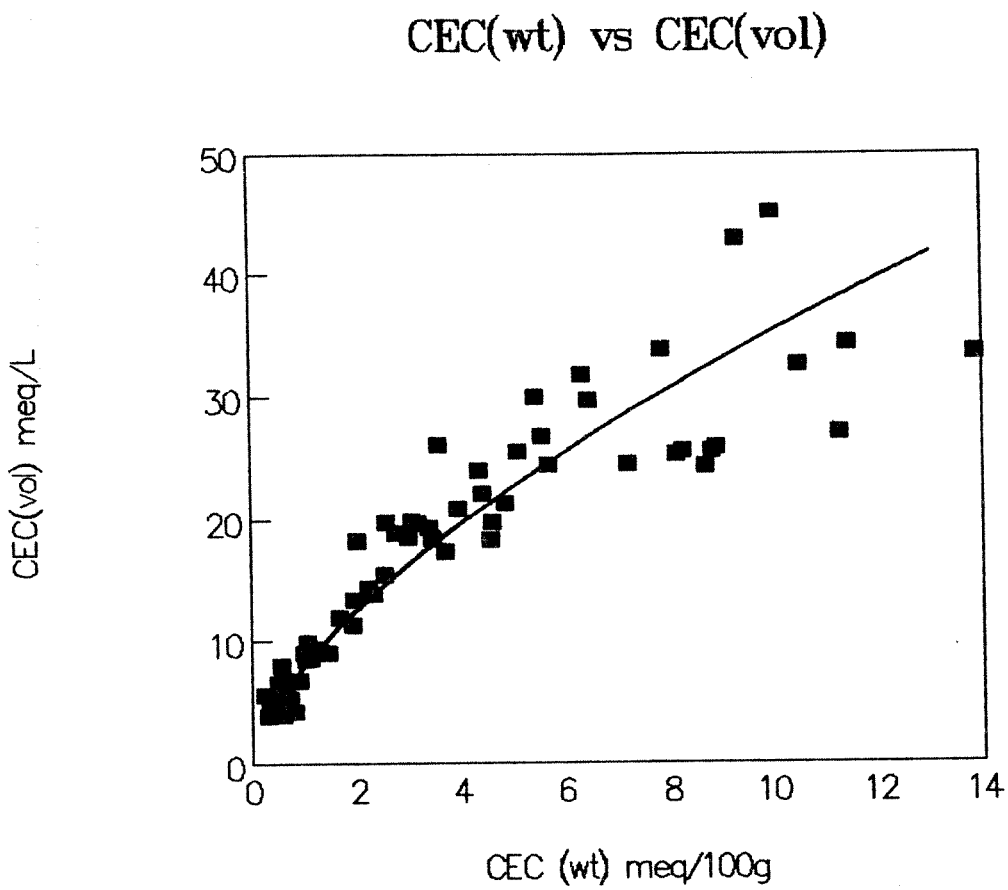


Figure 4.2. Sogndal. The relationship between CEC by weight and CEC by volume. The regression equation is $y = 8.125X^{-.6375}$, with an $r^2$ of 0.935.

## Part II. Risdalsheia

### 1. RELATIONSHIPS WITH CARBON CONTENT

#### 1.1 Loss on Ignition versus Percent Carbon

At Risdalsheia the relationship of loss on ignition to carbon is very close as was the case at Sogndal (Figure 1.1). The regression equation in this case is:

$$Y = 1.52 + 1.87x, \quad r^2 = 0.963, \; n = 115 \qquad (2.1)$$

The slope indicates that 1/1.87, or 53% of the weight loss on ignition is carbon, very near the 51% value observed for the Sogndal site.

#### 1.2 CEC(KCl) versus Percent Carbon

Again this relationship (Figure 1.2) is very close. The regression line is:

$$Y = 1.08 + 0.702x, \quad r^2 = 0.91 \qquad (2.1)$$

Four points on the low side of the line are all from the 1984 sampling, and these were excluded from the regression, on the basis that the general relationship is probably better described in this manner. If these points are included the $r^2$ is 0.852, and the slope is 0.658.

The slope suggests a CEC at soil pH of about 0.70 meq/100g for every 1% carbon. This is above the 0.55 value found at Sogndal but still well below the 4.9 per 1% carbon suggested by Jackson (1968). Again the difference is probably largely due to use of an unbuffered method for CEC determination for these samples, as compared to methods buffered at pH 7.0 or higher which include substantial variable charge that is not available at soil pH.

## 2.0 CATION EXCHANGE CAPACITY (CEC)

In order to arrive at a single value for CEC, or a single value for each depth, the individual values must be aggregated. First the distributions were examined. These were highly skewed with a large influence from a few relatively high values. Normal probability plots were examined for the original data, log(base e) transformations and square root transformations. Examples for the original data and the log transforms are shown in Figure 2.1. Relevant statistics for each transform are shown in the Appendix.

While the most suitable transform varies with depth, the lognormal distribution was selected as most appropriate on an overall basis. The log transform was then used for analyses of variance and the geometric means reported. The means are summarized in Table 2.1.

With the lognormal distribution the confidence intervals are not symmetrical about the means, as these are calculated for the mean of the logs prior to taking the antilogs.

The CEC values at this site are more than double those found at Sogndal. Samples were taken from the 0-15 cm, 15-30 cm, and in some cases, from 30-45 cm. An overall estimate and a separate estimate for each depth are calculated. Because there are only about half as many samples from 30-45 cm as from the other depths, a value for > 15 cm is also given, which includes all samples from 15-30 and 30-45 cm. Depth differences are highly significant (Figure 2.2), with progressively lower values as depth increases. The largest change occurs between the 0-15 cm and 15-30 cm depths.

Again, there is a significant difference among years (Figure 2.2). The pattern differs from that observed at

Sogndal, in that while the 1983 samples tend toward high values at both sites, at Risdalsheia the 1986 values are also high, while at Sogndal the 1986 values were similar to those from 1984 and 1985. There seems to be no rational basis for rejecting any of the data sets, so values from all four years are used both for aggregation of CEC and for calculation of the base cation saturation values.

## 3.0 BASE SATURATION

### 3.1 Ca and Mg Saturation

As is evident from Figure 3.1, there is a very close relationship between exchangeable Ca and Mg at this site. The equation for the regression of Mg on Ca (zero intercept) is,

$$y = 0.53x, \quad r^2 = 0.95 \qquad (4.1)$$

This close relationship was utilized in the estimation of the values for Ca and Mg saturation. First, the total saturation of (Ca+Mg) was calculated and aggregated by depth. Again, the distribution was highly skewed, and the lognormal distribution was selected. Geometric means and confidence intervals are shown in Table 3.1. The estimates of Ca and Mg saturation shown in Table 3.2 were then based on a Mg:Ca ratio of 0.53:1, as indicated by the slope of 0.53 for the regression of Mg on Ca.

The overall Ca saturation is only about one-third that observed at Sogndal, with the greatest difference at the deeper depths. Ca saturation in the 0-15 cm layer at Sogndal is estimated at 0.183, about 1.6 times the Risdalsheia value. The Sogndal value for > 15 cm is 0.168, more than five times the Risdalsheia value. Year effects are again very difficult to interpret. As noted in section 2, there was an apparent rise in CEC, with high values in 1983 and 1986. Also there were low values for exchangeable Ca+Mg in 1985 and high values in 1986 (Figure 3.2). These

effects appear to be an artifact of the measurement process, but the exact source is unknown.

### 3.2 K saturation

The K saturation values as estimated using the various distributions were quite similar. The log normal distribution was again selected on the basis of the linearity of the Normal Probability plots. Geometric means and confidence intervals are shown in Table 3.3.

The K saturation value for the 0-15 cm depth is 0.028, about the same as the value of 0.03 obtained for all depths at the Sogndal site. At Risdalsheia, however, the K saturation is clearly lower in the deeper layers, with a geometric mean of 0.015 for all values below 15 cm.

### 3.3 Na Saturation

Again a single Na saturation value is derived for all depths. This is based on the regression of exchangeable Na on CEC, as shown in Figure 3.3. In this case the intercept of the regression is not significant, and Na saturation value is taken from the slope of the regression with zero intercept. The regression equation is,

$$y = 0.0140x, \quad r^2 = 0.70 \qquad (4.2)$$

The estimate of Na saturation is given by the slope, i.e. 0.014. The standard error of the slope is 0.00043, and there are 114 observations. Given the low Na saturation, no attempt was made to separate the observations by depth. However, the lack of any evidence for either an intercept or non-linearity suggests that any depth effects would be small. The points at the lower left of a graph such as Figure 3.3 tend to be from the deeper layers where cation exchange capacity is low. If the saturation decreases with depth these points tend to be below a straight line with origin at zero, resulting in a negative intercept.

Conversely an increase in saturation with depth tends to give a positive intercept.

## 4.0 DENSITY

There appeared to be little clear advantage for any of the distributions for estimating densities. Geometric means were selected largely on the basis of consistency with the other parameters for this site. These are shown in Table 4.1. Densities at this site are lower than at Sogndal, particularly at the 0-15 cm depth where the density at Risdalsheia is 0.221 kg/l, compared to 0.511 kg/l at Sogndal.

## 5.0 SUMMARY

A summary table (5.1) for the Risdalsheia site has been prepared showing the best estimates for the aggregated values of the parameters required by the MAGIC model. While these may change with further analysis of these or later data, the modifications are likely to be relatively small.

Table 2.1. Risdalsheia. Geometric means and confidence intervals for CEC (KCl).

| Depth | n | Geometric mean | Confidence interval +/- 2(s.e.) |
|---|---|---|---|
| cm | | - - - - - - meq/100g - - - - - - | |
| All | 115 | 8.22 | 7.27 - 9.30 |
| 0-15 | 46 | 13.94 | 12.52 - 15.52 |
| 15-30 | 46 | 6.42 | 5.96 - 6.92 |
| 30-45 | 23 | 4.66 | 3.54 - 4.66 |
| > 15 | 69 | 5.75 | 5.01 - 6.61 |

Table 3.1. Risdalsheia. Geometric means and confidence intervals for (Ca+Mg) saturation.

| Depth | n | Geometric mean | Confidence interval +/- 2(s.e.) |
|---|---|---|---|
| cm | | meq/100g | |
| All | 115 | 0.082 | 0.069 - 0.098 |
| 0-15 | 46 | .171 | .150 - .194 |
| 15-30 | 46 | .054 | .042 - .070 |
| 30-45 | 23 | .049 | .034 - .071 |
| > 15 | 69 | .051 | .041 - .063 |

Table 3.2. Risdalsheia. Estimates of Ca and Mg saturation, assuming a Mg:Ca ratio of 0.53.

| Depth | Exch. Ca | Exch Mg |
|---|---|---|
| cm | meq/100g | meq/100g |
| All | 0.054 | .028 |
| 0-15 | .112 | .059 |
| 15-30 | .035 | .019 |
| 30-45 | .032 | .017 |
| > 15 | .033 | .018 |

Table 3.3. Risdalsheia. Geometric means and confidence intervals for K saturation.

| Depth | n | Geometric mean | Confidence interval +/- 2(s.e.) |
|---|---|---|---|
| cm | | meq/100g | |
| All | 114 | 0.019 | 0.018 - 0.021 |
| 0-15 | 46 | .028 | .026 - .030 |
| 15-30 | 46 | .016 | .014 - .018 |
| 30-45 | 22 | .013 | .013 - .016 |
| > 15 | 68 | .015 | .013 - .016 |

Table 4.1. Risdalsheia. Geometric means and confidence intervals for density (kg/l).

| Depth | n | Geometric mean | Confidence interval +/- 2(s.e.) |
|---|---|---|---|
| cm | | - - - - - - - kg/l | - - - - - - - |
| All | 80 | 0.401 | 0.336 - 0.479 |
| 0-15 | 35 | .221 | .179 - .273 |
| 15-30 | 33 | .630 | .517 - .768 |
| 30-45 | 12 | .656 | .477 - .902 |
| > 15 | 45 | .637 | .539 - .752 |

Table 5.1. Summary table of aggregated values of soil parameters at the Risdalsheia site for use in the MAGIC model.

| Depth | Density | CEC | Base Saturation Ca | Mg | K | Na |
|---|---|---|---|---|---|---|
| cm | kg/l | meq/100g | ------Equivalent Fraction------ | | | |
| All | 0.401 | 8.22 | 0.054 | 0.028 | 0.019 | 0.014 |
| 0-15 | .221 | 13.94 | .112 | .059 | .028 | .014 |
| 15-30 | .630 | 6.42 | .035 | .019 | .016 | .014 |
| 30-45 | .656 | 4.66 | .032 | .017 | .013 | .014 |
| > 15 | .637 | 5.75 | .033 | .018 | .015 | .014 |

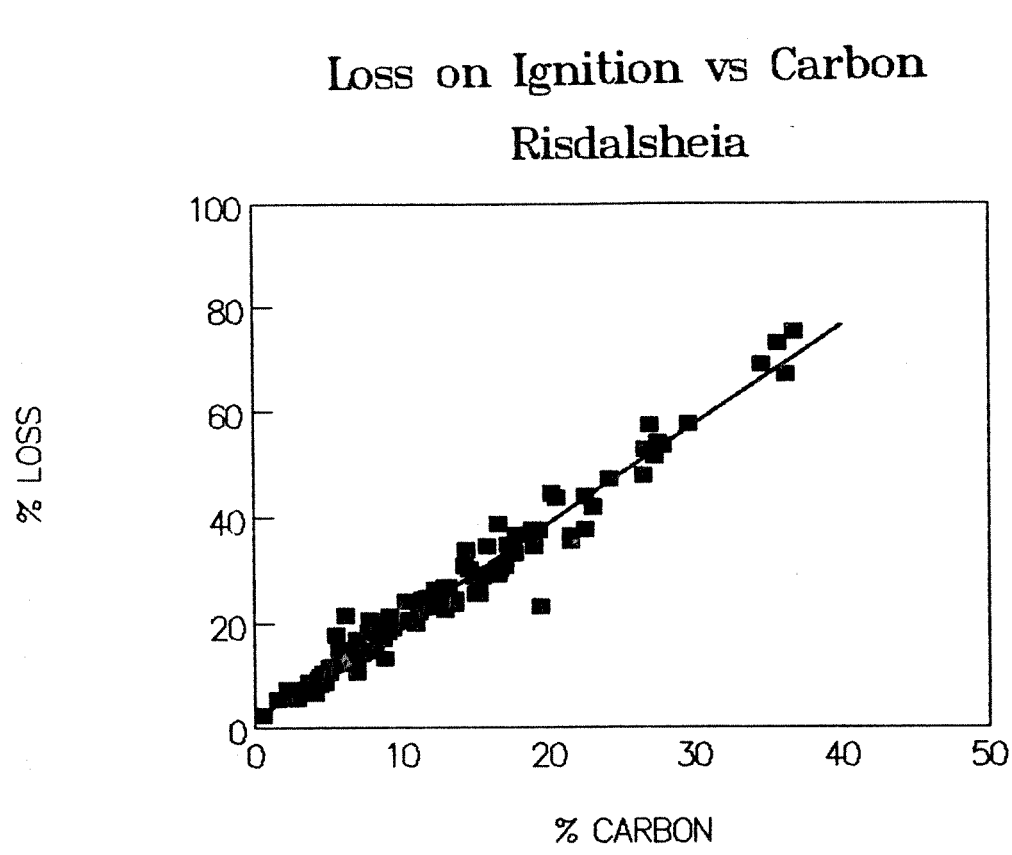


FIGURE 1.1. Risdalsheia. Loss on ignition as a function of percent carbon as determined by a chromic acid wet digestion.

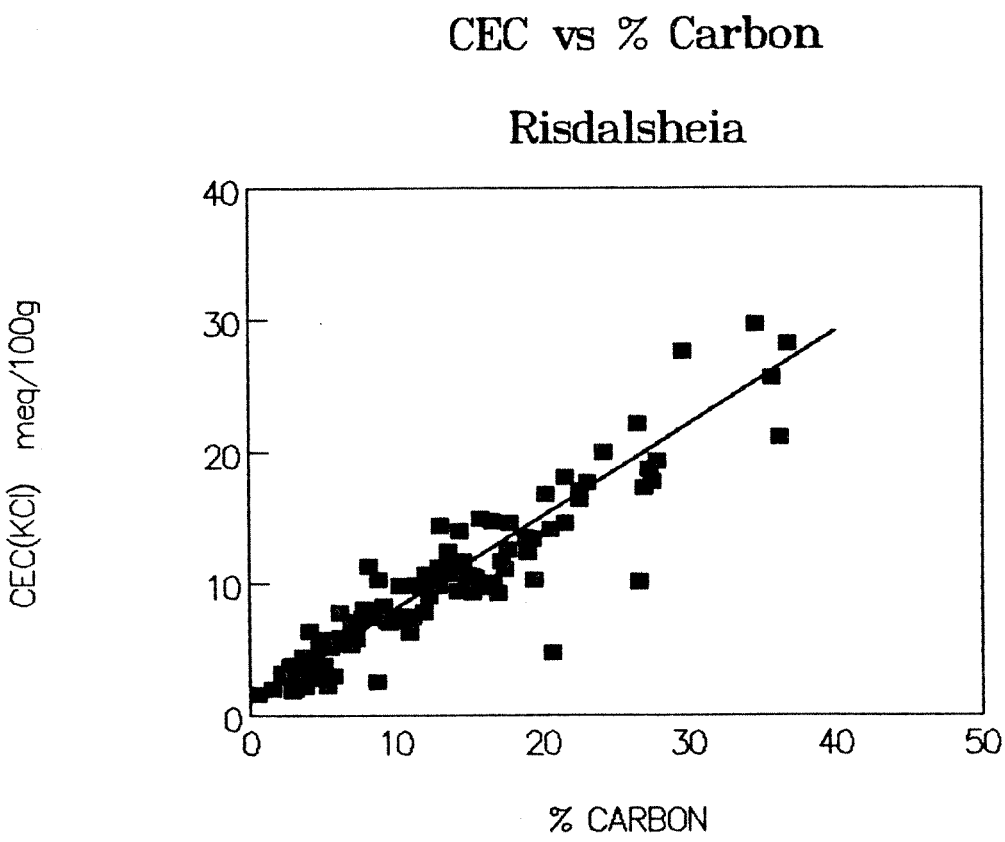


FIGURE 1.2. Risdalsheia. Cation exchange capacity (KCl) in meq/100g as function of percent carbon.

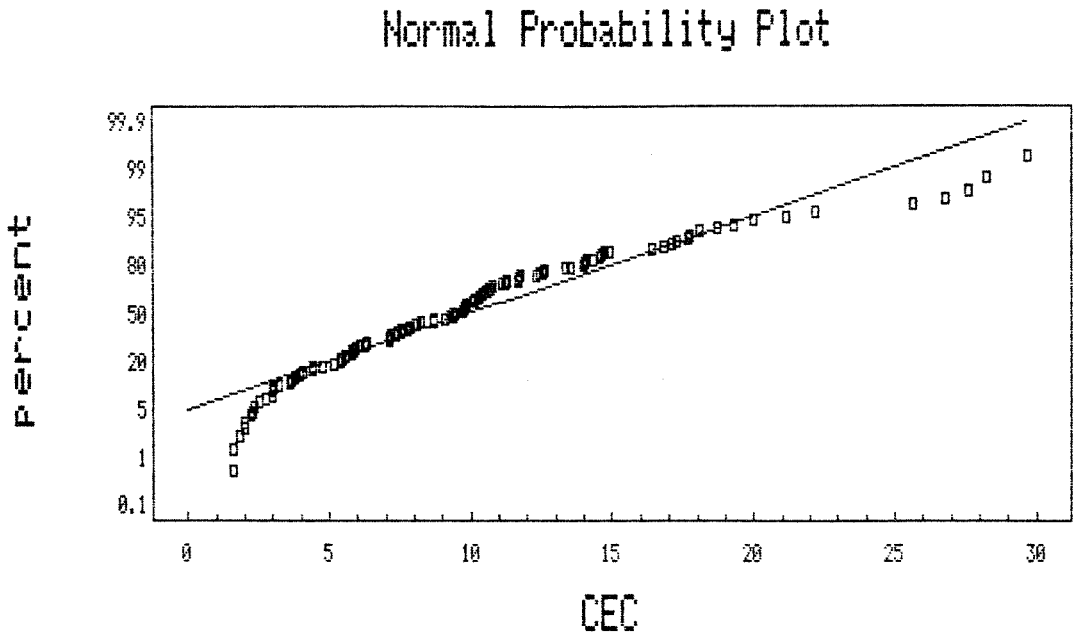


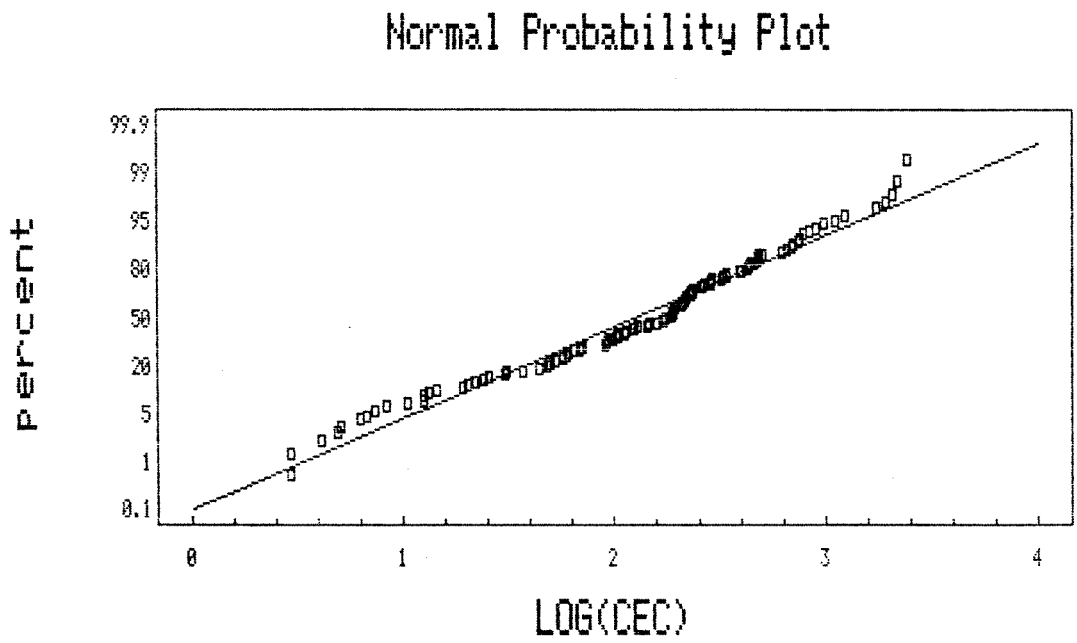


FIGURE 2.1. Risdalsheia. Normal probability plots for cation exchange capacity by weight, and for the log transform of the same data.

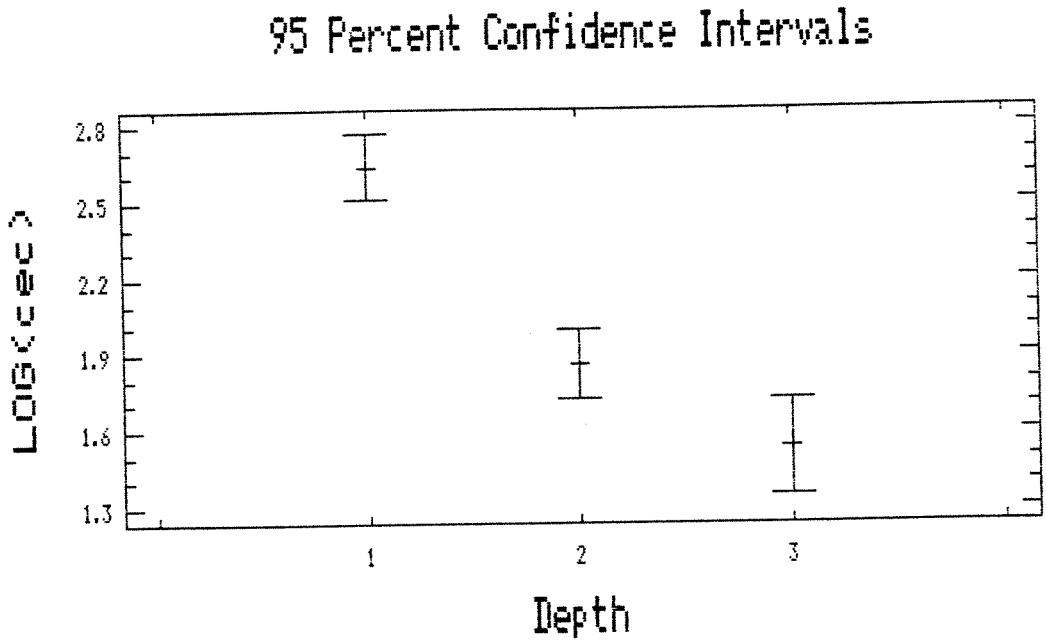


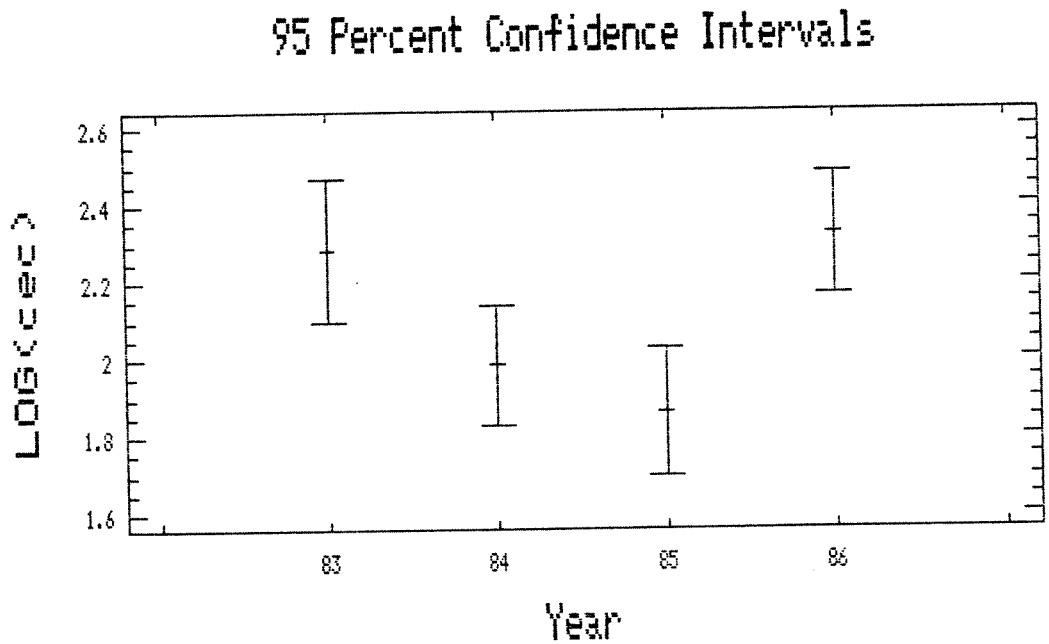


FIGURE 2.2. Risdalsheia. Means plots showing the 95% confidence interval for the logarithm (base e) of CEC by depth and year.

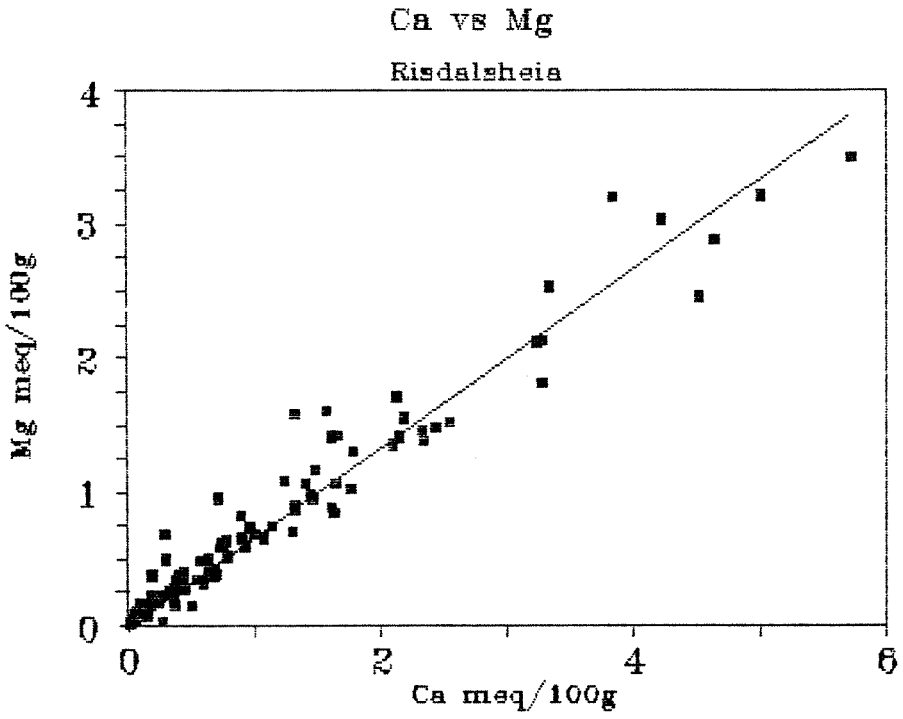


FIGURE 3.1. The relationship between exchangeable Ca and Mg at Risdalsheia. The slope (no intercept) is 0.53 and the $R^2$ value 0.95.

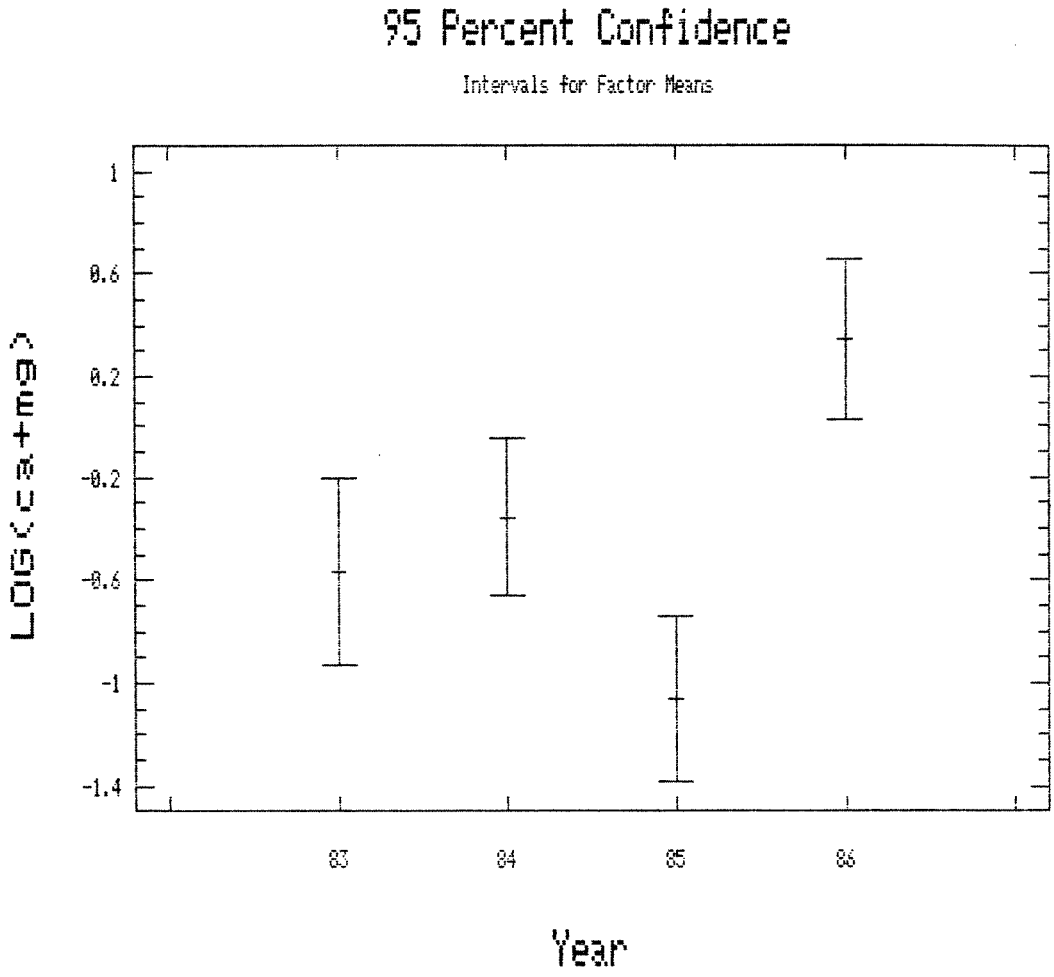


FIGURE 3.2. Risdalsheia. Means plots showing the 95% confidence interval for the logarithm (base e) of exchangeable (Ca+Mg) by years.

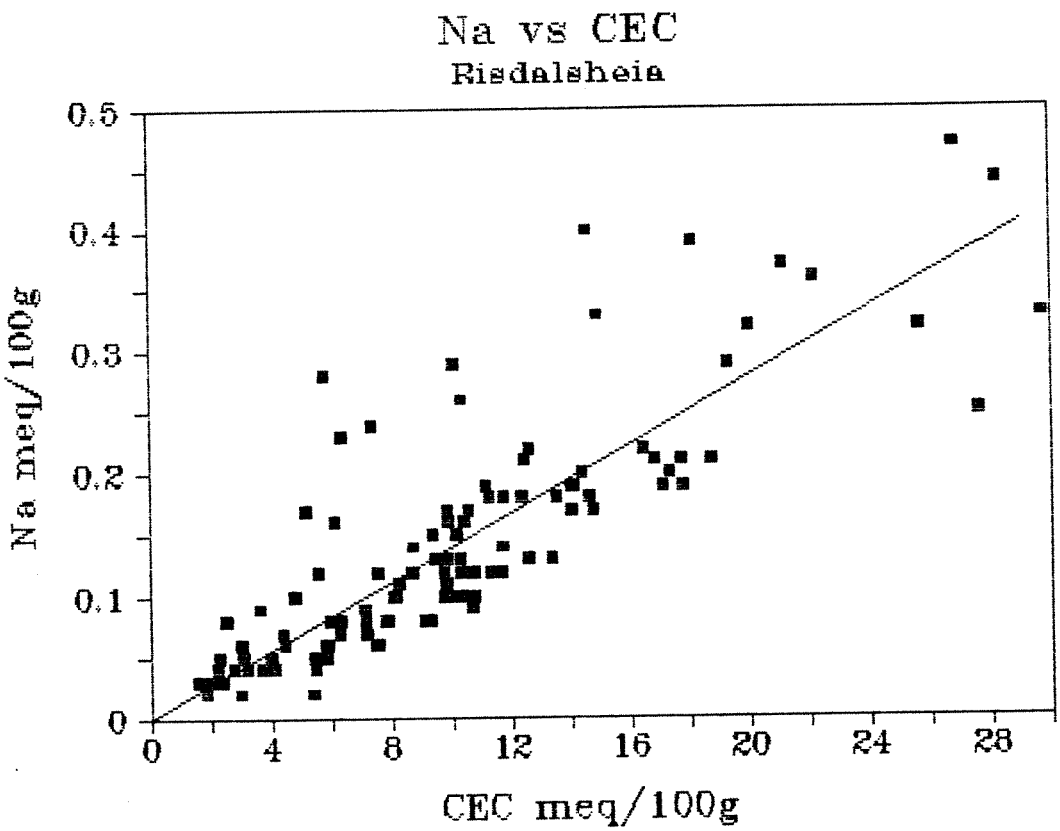


FIGURE 3.3. Risdalsheia. Regression of exchangeable Na on CEC. The slope (no intercept) of 0.014 estimates the Na saturation. $R^2$ is 0.70.

## Part III. Anion adsorption.

### 1.0 INTRODUCTION

This part deals with the $Cl^-$ and $SO_4^{2-}$ adsorption properties of soil samples from Risdalsheia and Sogndal. These anion adsorption properties serve to buffer changes in anion concentrations of water as it passes through the soil. This buffering effect creates a lag in changes of concentration of drainage waters as compared to concentration of inputs in precipitation or dryfall. These lags, in turn, affect the response of surface waters to deposition inputs.

Anion adsorption properties are commonly described in terms of an "isotherm", i.e. a plot or mathematical function describing the amount of the adsorbed ion present as a function of the concentration of the ion in solution. While any of a number of mathematical expressions may be used to describe this relationship, the linear isotherm and the "Langmuir" isotherm will be applied here. The simplest case is the linear isotherm, for which the amount adsorbed is directly proportional to the solution concentration. For example,

$$Cl^-_{ads} = b(Cl^-), \qquad (1.1)$$

where $Cl^-_{ads}$ represents the amount adsorbed, usually expressed in mg/kg or meq/kg, and $(Cl^-)$ represents the solution concentration, usually expressed in mg/l or meq/l. The change in the amount in the adsorbed phase per unit of concentration change is given by the slope, b.

The Langmuir isotherm is commonly used to describe $SO_4^{2-}$ adsorption and may be described by,

$$S_{ads} = \frac{K_{max}(S)}{K_{1/2} + (S)} \qquad (1.2)$$

where $K_{max}$ represents the maximum amount that can be adsorbed, i.e. the amount adsorbed at infinite solution concentration, while $K_{1/2}$ represents the solution concentration at which the amount adsorbed is equal to one-half $K_{max}$. The use of Eq. (1.2) implies the existence of an "adsorption maximum", i.e. an adsorbed amount that will not be exceeded at any solution concentration. Eq. (1.2) is also written in terms of S rather than $SO_4^{2-}$, because in most cases the data used in this report are expressed in terms of mg S/kg for the adsorbed phase and mg S/l for concentration.

## 2.0 METHODS

The samples used to determine anion adsorption properties were collected and analyzed under the supervision of Dr. Erik Lotse at the Swedish Agricultural University in Uppsala (Lotse and Ottabong 1985, Lotse 1989). In general, the $Cl^-$ adsorption data were obtained by equilibrating wet soil samples (approximately 2.5 gm dry soil equivalent) with 25 ml of solution with initial concentrations of 0, 8, 16, and 32 mg $Cl^-$ per liter, and determining the $Cl^-$ concentration after equilibration. The amount adsorbed or desorbed is then calculated from the change in concentration. For the sulfate adsorption isotherms equilibration solutions containing 0, 1, 2, 4, 8, 16, and 32 mg S/l were used.

The observed $Cl^-$ isotherms were very nearly linear, and no attempt was made to describe them in terms of the Langmuir-type relationship. Similarly, because most of the plots for the $SO_4^{2-}$ isotherms at the Risdalsheia site appeared linear, a linear isotherm was used and no attempt was made to describe these using the Langmuir relationship. Some curvilinearity was observed for several of the $SO_4^{2-}$ isotherms for the Sogndal site, and in these cases the constants for the Langmuir relationship were estimated.

Concentrations determined after equilibration differ from those determined before equilibration by the amount of the ion that has been desorbed or adsorbed during the equilibration process. At low initial concentration the solution becomes more concentrated due to desorption, while at higher concentrations, adsorption occurs and the solution becomes less concentrated. The procedure used here was to convert this change in concentration (- for desorbed and + for adsorbed) to units of mg/kg and plot this change against final concentration. An example using the $Cl^-$ data from the 0-15 cm depth at sampling site #2 at Sogndal is shown in the upper graph in Figure 2.1. The linear regression relationship for this plot is,

$$Y = -6.43 + 1.223X, \; r^2 = 0.988 \qquad (2.1)$$

Not all the relationships are this close, and in a few cases obvious outliers were deleted before calculating the regressions. Since the relationship is linear, the intercept of -6.43 mg/kg represents the amount that would have to be desorbed in order to achieve a zero final concentration, i.e. the total amount adsorbed assuming full reversibility of adsorption. Therefore, in order to construct an isotherm showing the amount adsorbed as a function of final solution concentration, the curve must be displaced upward by 6.43 mg/kg, i.e, 6.43 mg/kg must be added to each observed value. When this is done the isotherm passes through 0,0 as required by Eq. (1.1). and shown in the lower graph in Figure 2.1.

The equilibrium concentration is given by the concentration at which no $Cl^-$ is adsorbed or desorbed, i.e. the concentration at which the curve for the lower graph in Figure 2.1 intercepts the Y axis. From Eq. (2.1) we may calculate this equilibrium concentration for our example to be 5.26 mg/kg.

The slope is the key parameter for a linear isotherm. It represents the change in adsorbed phase (mg/kg in this case) per unit of concentration change. A steep slope means that there will be a large change in adsorbed phase for a small change in solution concentration, i.e. the system will be well buffered against changes in solution concentration. Conversely, a flatter slope is associated with less buffering due to the adsorption process.

The procedure used here is slightly different from that which was previously used to construct isotherms from these data. In the previous scheme all final concentrations were adjusted by subtracting the concentration observed after equilibration with solutions of zero initial concentration. This is equivalent to adjusting by the amount desorbed when equilibrated with the solution of initial concentration of zero rather than extrapolating to the amount that must be desorbed to equilibrate with a final concentration of zero. The differences are usually rather small, in our example the adjustment by the previous procedure would have been about 4.52 mg/kg rather than the 6.43 mg/kg arrived at by extrapolation. However, in some cases the differences may be significant and the extrapolation procedure used here appears to be more appropriate.

Two methods have been tried for fitting the Langmuir isotherm in the form shown in Eq. (1.2). It is apparent from Eq. (1.2) that at very low concentrations the function approaches linearity, as when (S) is small in relation to $K_{1/2}$, the (S) term in the denominator becomes insignificant and the function approaches,

$$S_{ads} = \frac{K_{max}(S)}{K_{1/2}} \qquad (2.2)$$

Thus, if only points from the low end of the solution concentration are used, a linear extrapolation to zero concentration should be appropriate. This was done by simply visually inspecting the original plot of

adsorbed/desorbed and selecting a cutoff point below which the curve was apparently linear. An example of such a plot for the $SO_4^{2-}$ data from sampling site #9 at Sogndal is shown in the upper graph in Figure 2.2. Linear regression was then used to extrapolate these points to zero final concentration. In the case of the example the cutoff was set at an initial concentration of 8 mg S/kg for both depths. However, in several instances the cutoff was set at an initial concentration of 4 mg S/kg to avoid the non-linear portions of the curve. For the example shown in Figure 2.2 the extrapolations yielded initial values of -20.17 and -10.64 mg S/kg for the 0-15 and 15-30 cm depths, respectively, and these values were used to adjust the adsorbed values before proceeding to the next step in the fitting procedure.

By inverting Eq. (1.2) and rearranging we obtain,

$$\frac{1}{S_{ads}} = \frac{K_{1/2}}{K_{max}\ (S)} + \frac{1}{K_{max}} \qquad (2.3)$$

From Eq. (2.3) it is apparent that if the relationship in Eq. (1.2) applies, a plot of $1/S_{ads}$ as a function of $1/(S)$ should be linear, and the intercept is the reciprocal of $K_{max}$. Once $K_{max}$ is known $K_{1/2}$ may be calculated from the slope. A reciprocal plot for the Sogndal site #9 example is shown in the lower graph in Figure 2.2. The curvelinearity of the adsorption curve is determined largely by the points at high concentrations, which are the points at the lower left of the reciprocal curve. The low concentration points, particularly those with an initial concentration of zero were sometimes inconsistent on the reciprocal plot. This inconsistency may arise simply due to measurement error, as at very low concentrations small differences will have a large effect on the reciprocal. Similarly, small differences due to errors in the extrapolation used to calculate the correction for the

native adsorbed phase would cause large differences in the reciprocals. Therefore, the fitting of Eq. (2.3) was confined to points with initial concentration (prior to equilibration) of 2.0 mg S/l or greater. The slopes and intercepts of the reciprocal curve were then determined by linear regression, and $K_{max}$ and $K_{1/2}$ were calculated. Results for the example are shown in Table 2.1.

The adsorption plot for the 0-15 cm depth is nearly linear, and this is reflected in the relatively large values for $K_{max}$ and $K_{1/2}$.

Again, the equilibrium concentration is the concentration at which no change in adsorption takes place, i.e. the concentration at which the uncorrected adsorption curve has a value of zero. Defining our correction values obtained from the intercepts (in our example 20.17 and 10.64 mg S/kg for the 0-15 and 15-30 cm depths respectively) as C, Eq. (1.2) for the uncorrected adsorption values may be written as,

$$S_{ads}\ (\text{uncorrected}) = \frac{K_{max}(S)}{K_{1/2} + (S)} - C \qquad (2.4)$$

Setting $S_{ads}$ (uncorrected) equal to zero we may solve for the equilibrium concentration, $(S)_{eql}$,

$$(S)_{eql} = \frac{K_{1/2}C}{K_{max} - C} \qquad (2.5)$$

The second procedure used for fitting Eq. (2.2) involves the use of a non-linear regression program for curve fitting. Equation (2.2) must go through the origin. However, if a constant C is added Eq.(2.2) takes the form,

$$S_{ads} = C + \frac{a(S)}{b + (S)} \qquad (2.6)$$

The constant C represents the correction for the adsorbed phase that must be applied to bring the curve to a zero intercept. When a non-linear regression program is used to fit this curve the intercept is -C, which represents the extrapolation of the Langmuir relationship to zero concentration. When this correction is applied and the curve is refit, C is very nearly zero while a and b are direct estimates of $K_{max}$ and $K_{1/2}$, respectively. The equilibrium concentration may then be calculated using Eq. (2.5).

An example of the fitted isotherm for the 15-30 cm depth at sampling site #9 at Sogndal is shown in Figure 2.3. In this case the correction as calculated by the non-linear regression was 11.94 mg/kg as compared to 10.64 mg/kg as calculated above by linear extrapolation of the low concentration points. In principle this procedure should estimate this correction more accurately than the linear extrapolation, particularly if the relationship is markedly curvilinear. In this case the estimated values of $K_{max}$ and $K_{1/2}$ are 250 mg S/kg and 50.2 mg/l, respectively. These compare to respective values of 244 mgS/kg and 51.5 mg/l as calculated using the reciprocal procedure above (Table 2.1).

## 3.0 CHLORIDE ADSORPTION

### 3.1 Risdalsheia

An example of a $Cl^-$ isotherm from Risdalsheia is shown in Figure 3.1. The "Initial" isotherm has not been corrected for the adsorbed phase, and the intercept is used to estimate the amount in the adsorbed phase in the original sample. In the "Final" isotherm this amount has been added to the observed amount in each sample, so that the isotherm starts at zero concentration and zero adsorbed $Cl^-$.

The isotherm characteristics for the two depths are shown in Table 3.1. The constant (intercept), slope and $r^2$ were

determined using linear regression. The slope represents the amount (mg/kg) that must be adsorbed/desorbed for the concentration to change by one mg/l. While all calculations were made using these units, the slope would be the same for units of meq/kg and meq/l. The amount of adsorbed $Cl^-$ present (negative of the constant) is about three times as high in the 0-15 cm layer as in the 15-30 cm layer. The slope is also greater at 0-15 cm, indicating that on a weight basis, more $Cl^-$ must be adsorbed or desorbed for a given change in solution concentration. The density is lower in the 0-15 cm depth, so on a volume basis these differences would largely disappear. The equilibrium concentrations are also higher at 0-15 cm than at 15-30 cm. It is not known whether this difference might be permanent, or temporary due to high sea salt input prior to sampling. However, depth effects were much less apparent at the Sogndal site.

The mean equilibrium concentrations are 17.6 mg/kg and 9.12 mg/kg for the 0-15 cm and 15-30 cm depths, respectively. If these isotherms were to accurately reflect the field system, the drainage water $Cl^-$ concentration would be approximately the same as the equilibrium concentration. However, volume weighted mean runoff concentrations at Risdalsheia average about 105 ueq/l (Wright et al. 1988), or about 3.7 mg/l. This is less than one-half the mean equilibrium concentration as calculated from the isotherm data for the 15-30 cm depth and less than one-fourth that for the 0-15 cm depth.

### 3.2 Sogndal

Sample isotherms for the Sogndal site are shown in Figure 2.1. Isotherm characteristics are shown in Table 3.2. The slopes are quite similar for the two sites, but the initial amounts adsorbed are lower at Sogndal than at Risdalsheia. Also there is little or no indication of any difference due to depth at Sogndal. Mean equilibrium concentrations are 4.58 mg/l at the 0-15 cm depth and 3.70 at 15-30 cm. These

are only about half the concentration at the 15-30 cm depth at Risdalsheia. Again, this is well above the volume weighted mean of about 1.46 mg/l for runoff at Sogndal during the 1983-87 period (Wright et al. 1988). However, mean $Cl^-$ concentrations in runoff vary by 2-3 times from year-to-year at Sogndal, and the mean for the four catchments was 2.52 mg/l during the 1984 season (Wright et al. 1988).

## 4.0 SULFATE ADSORPTION

### 4.1 Risdalsheia

The $SO_4^{2-}$ isotherms at Risdalsheia were generally very nearly linear. There did seem to be some tendency toward non-linearity at the 0-15 cm depth, but this was not sufficient to allow fitting of the Langmuir relationship. However, because of the geometric increase in concentrations of the equilibrating solutions, in a linear regression these high points exert a substantial influence on the slope and intercept. As the accurate extrapolation of the intercept to zero final concentration is critical in establishing the correction for native adsorbed $SO_4^{2-}$, the points from the initial concentration of 32 mgS/l were not used for the regressions at the 0-15 cm depth. At site #12 the 8 mg/l solutions were also excluded.

Example isotherms from sampling site #10 (KIM) catchment are shown in Figure 4.1, and the isotherm characteristics are summarized in Table 4.1. As was the case with $Cl^-$, on a weight basis there is substantially more adsorbed $SO_4^{2-}$ at the 0-15 cm depth than at 15-30 cm. The means are 24.02 mg S/kg at 0-15 cm and 9.43 mg S/kg at 15-30 cm. Also, the estimated equilibrium concentrations are substantially higher than those found in drainage water at the site. For example, the mean equilibrium concentration for the 15-30

cm depth is 7.06 mg S/kg or about 440 ueq/l. This exceeds weighted annual mean sulfate concentrations in runoff at EGIL catchment (roofed, acid rain) by about a factor of four (Wright et al. 1988).

It is also of interest to compare the amounts of adsorbed $SO_4^{2-}$, as estimated from extrapolating the isotherms, with independent measurements of "soluble" sulfate as measured by a water extraction and "adsorbed" sulfate as measured by a phosphate extraction following water extraction, as shown in Table 4.2. It is apparent that the estimates from the isotherms are similar to those from the water extraction. This is not surprising as the procedures are quite similar. However, it also appears that the additional adsorbed $SO_4^{2-}$ that is removed by the phosphate extraction does not participate in the adsorption/desorption process, at least as measured by the isotherm.

4.2 Sogndal

The $SO_4^{2-}$ isotherms for the Sogndal site were fit to the Langmuir isotherm using both a reciprocal plot procedure and non-linear regression. Isotherm characteristics as determined by the two methods are shown in Tables 4.3 and 4.4, respectively. In a few cases the Langmuir relationship could not be applied as the isotherm was too nearly linear. As the curvilinearity was modest in all cases, these fitting procedures were used largely to demonstrate the methods. However they do give appropriate values for the native adsorbed sulfur (i.e. the constant) and for the equilibrium concentration. No judgement can be made as to the relative merits of the methods, as the data are too nearly linear. In most cases results are very similar. However, in one case the $K_{1/2}$ and $K_{max}$ values as determined by the non-linear regression appear to be very large. Within the range of the data points, however, there is very little difference in the actual isotherms.

At the moment no comparison can be made between the water extractions and the phosphate extractions, as these have not been summarized. Equilibrium concentrations are generally of the order of 3.0 mg/l (48 ueq/l). This is somewhat higher than the observed values of 20-30 ueq/l in runoff from the untreated reference catchments at Sogndal (Wright et al. 1988).

## REFERENCES

Cosby, B.J., G.M. Hornberger, J.N. Galloway, and R.F. Wright. 1985. Modelling the effects of acid deposition: assessment of a lumped-parameter model of soil water and streamwater chemistry. Water Resour. Res. 21: 51-63.

Jackson, M.L. 1958. Soil Chemical Analysis. Prentice Hall Inc. Englewood Cliffs NJ. 206p.

Lotse, E. G. 1989. Soil chemistry 1983-86 at the RAIN project catchments. Acid Rain Research Report 18/89. Norwegian Institute for Water Research. Oslo. 24 p.

Lotse, E., and E. Ottabong. 1985. Physiochemical properties of Soils at Risdalsheia: RAIN Project. Acid Rain Research Report 8/1985. Norwegian Institute for Water Research. Oslo. 48p.

Wright, R.F., E. Lotse, and A. Semb. 1988. Reversibility of acidification shown by whole-catchment experiments. Nature 334: 670-675.

## ACKNOWLEDGEMENTS

This work was conducted on contract to NIVA as part of the RAIN project. The RAIN project receives financial support from the Norwegian Ministry of Environment, The Royal Norwegian Council for Scientific and Industrial Research, the Ontario Ministry of the Environment, Environment Canada, the Swedish Environmental Protection Board, the Central Electricity Generating Board (UK), and from internal research funds from the participating institutes.

Table 2.1. Regression of $1/S_{ads}$ versus 1/(S) and calculated values of $K_{max}$ and $K_{1/2}$ for sampling site 9 at Sogndal.

| Depth cm | Intercept | Slope | $r^2$ | $K_{max}$ mg S/kg | $K_{1/2}$ mg S/l | Equil. mg S/l |
|---|---|---|---|---|---|---|
| 0-15 | 0.0015 | 0.175 | 0.993 | 668 | 116.7 | 3.63 |
| 15-30 | 0.0041 | 0.211 | 0.954 | 244 | 51.5 | 2.29 |

Table 3.1. Characteristics of the $Cl^-$ isotherms at Risdalsheia. The site numbers refer to sampling transects. Data are analyzed for KIM and EGIL catchments.

| Site/ Catchment | n | Constant mg/kg | $r_2$ | Slope | Equilibrium mg/L |
|---|---|---|---|---|---|
| 0-15 cm Depth | | | | | |
| 10/KIM | 8 | -51.63 | .950 | 2.74 | 18.8 |
| 12/KIM | 8 | -22.08 | .927 | 1.76 | 12.5 |
| 17-19/EGIL | 8 | -20.05 | .975 | 1.38 | 14.5 |
| 23-25/EGIL | 8 | -29.85 | .964 | 1.21 | 24.7 |
| mean | | -30.91 | | 1.77 | 17.6 |
| s.d. | | 14.44 | | .68 | 5.4 |
| 15-30 cm Depth | | | | | |
| 10/KIM | 8 | -12.46 | .878 | 1.69 | 7.4 |
| 12/KIM | 6 | -5.49 | .944 | .76 | 7.3 |
| 17-19/EGIL | 8 | -12.13 | .971 | 1.05 | 11.5 |
| 23-25/EGIL | 7 | -7.90 | .998 | .76 | 10.3 |
| mean | | -9.50 | | 1.07 | 9.1 |
| s.d. | | 3.38 | | .44 | 2.1 |

Table 3.2. Characteristics of the $Cl^-$ isotherms at Sogndal.

| Site | n | Constant mg/kg | $r_2$ | Slope | Equilibrium mg/l |
|---|---|---|---|---|---|
| 0-15 cm Depth | | | | | |
| 2 | 8 | -6.44 | .976 | 1.22 | 5.28 |
| 7 | 7 | -4.00 | .979 | 1.39 | 2.88 |
| 8 | 8 | -7.04 | .973 | 1.41 | 4.99 |
| 9 | 7 | -8.83 | .997 | 1.71 | 5.16 |
| | | mean | -6.57 | 1.44 | 4.58 |
| | | s.d. | 2.00 | .23 | 1.13 |
| 15-30 cm Depth | | | | | |
| 2 | 8 | -5.66 | .949 | 1.57 | 3.60 |
| 7 | 8 | -2.23 | .976 | 1.29 | 1.73 |
| 8 | 8 | -4.68 | .973 | .93 | 5.01 |
| 9 | 8 | -7.46 | .946 | 1.66 | 4.49 |
| | | mean | -5.00 | 1.36 | 3.70 |
| | | s.d. | 2.18 | .44 | 1.44 |

Table 4.1. Characteristics of the $SO_4^{2-}$ isotherms at Risdalsheia.

| Site/ Catchment | n | Constant mg S/kg | $r_2$ | Slope | Equilibrium mg S/l |
|---|---|---|---|---|---|
| 0-15 cm Depth | | | | | |
| 10/KIM | 12 | -17.10 | .930 | 2.67 | 6.37 |
| 12/KIM | 10 | -24.67 | .891 | 1.79 | 13.78 |
| 17-19/EGIL | 12 | -30.27 | .68 | 1.82 | 16.63 |
| 23-25/EGIL | 12 | -18.12 | .953 | 2.24 | 8.08 |
| | mean | -24.02 | | 2.13 | 11.47 |
| | s.d. | 6.60 | | .41 | 4.60 |
| 15-30 cm Depth | | | | | |
| 10/KIM | 14 | -9.02 | .966 | 1.39 | 6.49 |
| 12/KIM | 14 | -7.18 | .960 | 1.20 | 5.98 |
| 17-19/EGIL | 14 | -12.80 | .953 | 1.33 | 9.62 |
| 23-25/EGIL | 13 | -8.73 | .968 | 1.42 | 6.15 |
| | mean | -9.43 | | 1.34 | 7.06 |
| | s.d. | 2.39 | | .10 | 1.72 |

Table 4.2. Comparison of sulfate as estimated from extrapolation of the isotherms with that measured by water extraction followed by phosphate extraction.

| | 0 - 15 cm mg S/kg | > 15 cm mg S/kg |
|---|---|---|
| Water | 22.4 | 12.62 |
| Phosphate | 9.78 | 8.61 |
| Isotherm | 24.02 | 9.43 |

Table 4.3. Characteristics of the $SO_4^{2-}$ isotherm at Sogndal as fitted to the Langmuir isotherm using a reciprocal plot.

| Site/Field | Constant mg S/kg | $K_{max}$ mg S/kg | $K_{1/2}$ mg S/l | Equilibrium mg S/l |
|---|---|---|---|---|
| 0-15 cm | | | | |
| 2/(f2) | -29.46 | * | * | 10.73* |
| 7/(f2) | -14.61 | 140 | 24.5 | 2.85 |
| 8/(f4) | -13.73 | 169 | 51.4 | 4.55 |
| 9/(f1) | -20.16 | 668 | 116.7 | 3.63 |
| 15-30 cm | | | | |
| 2/(f2) | -26.84 | 318 | 98.6 | 9.09 |
| 7/(f2) | -14.20 | 142 | 25.0 | 2.78 |
| 8/(f4) | -11.29 | 814 | 280 | 3.94 |
| 9/(f1) | -10.64 | 244 | 51.5 | 2.35 |

* Parameters could not be calculated because isotherm essentially linear. Linear isotherm with slope of 2.74 used to calculate equilibrium concentration.

Table 4.4. Characteristics of the $SO_4^{2-}$ isotherm at Sogndal as fitted to the Langmuir isotherm using non-linear regression.

| Site/Field | Constant mg S/kg | $K_{max}$ mg S/kg | $K_{1/2}$ mg S/l | Equilibrium mg S/l |
|---|---|---|---|---|
| 0-15 cm | | | | |
| 2/(f2) | * | * | * | * |
| 7/(f2) | -15.82 | 210 | 24.5 | 2.85 |
| 8/(f4) | -13.44 | 270 | 58.1 | 3.04 |
| 9/(f1) | * | * | * | * |
| 15-30 cm | | | | |
| 2/(f2) | -26.55 | 11552 | 3928 | 9.05 |
| 7/(f2) | -14.57 | 316 | 92.0 | 4.45 |
| 8/(f4) | -12.27 | 225 | 66.0 | 3.81 |
| 9/(f1) | -11.97 | 254 | 50.0 | 2.47 |

* Parameters could not be calculated because isotherm essentially linear.

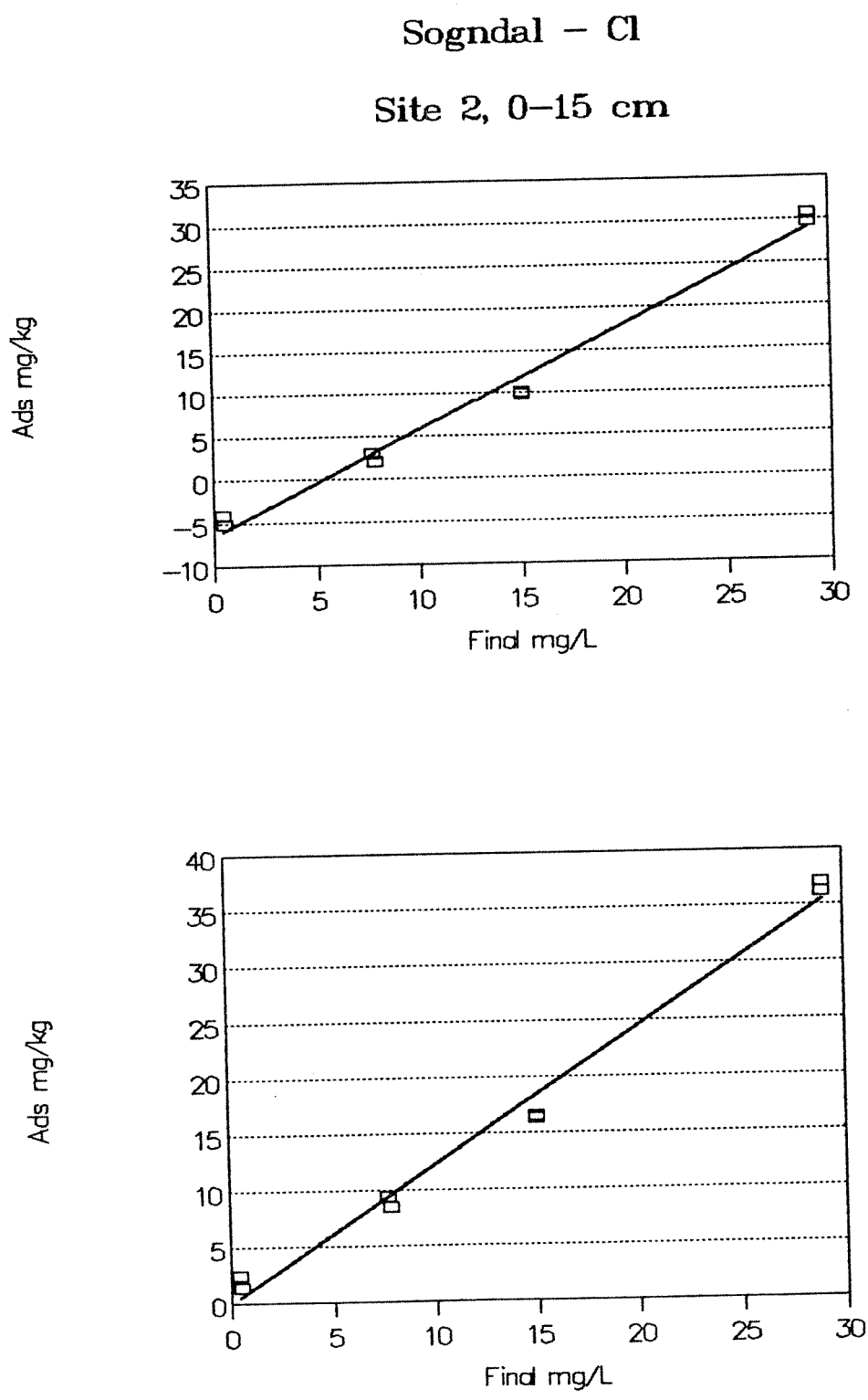


Figure 2.1. Initial uncorrected $Cl^-$ isotherm (above) and final corrected isotherm (below) for site 2 at Sogndal.

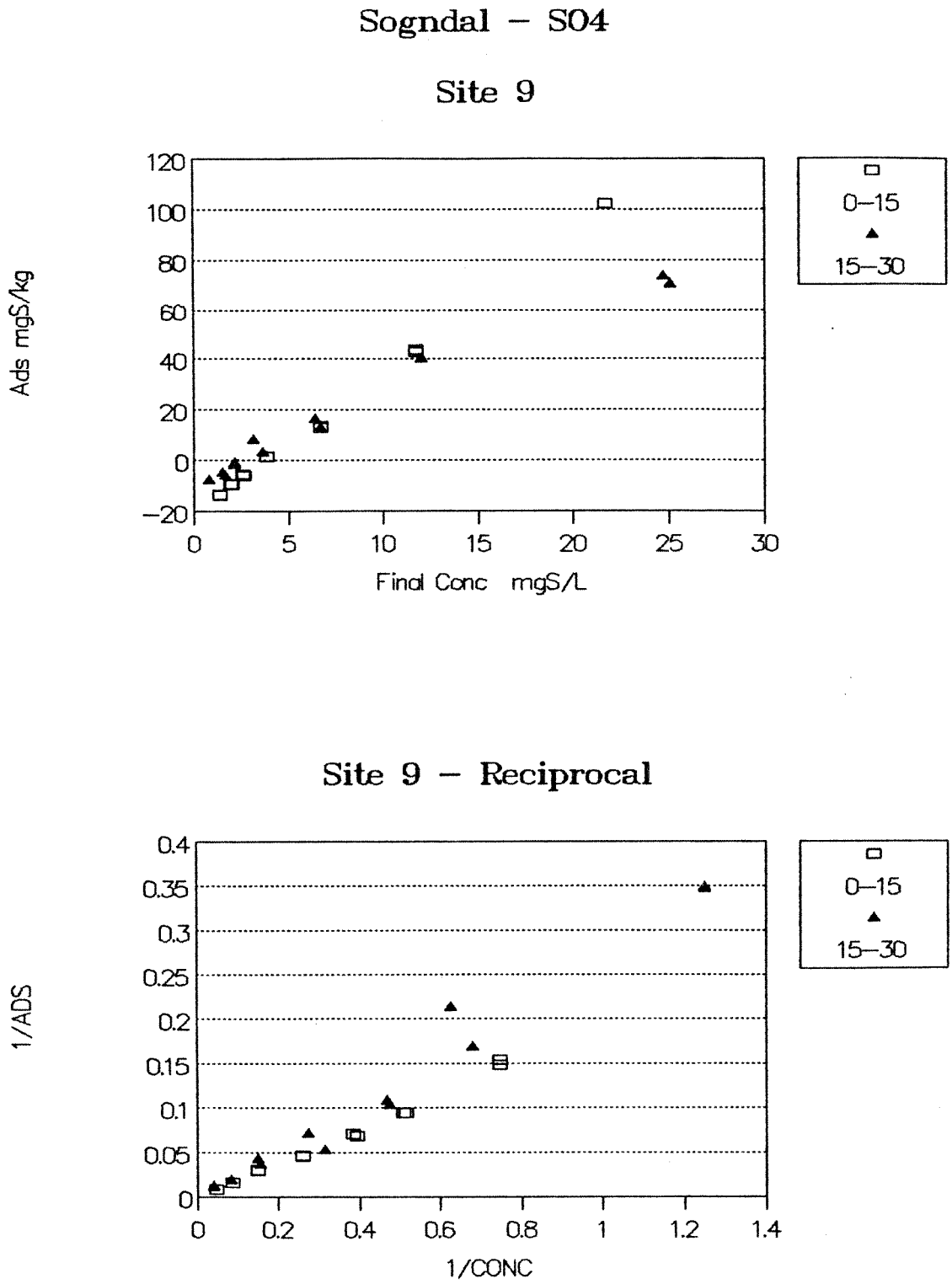


Figure 2.2. The initial uncorrected plot of $SO_4^{2-}$ adsorbed/desorbed (above) and reciprocal plot of corrected data used in fitting the Langmuir isotherm (below) for the 15-30 cm depth of sampling site 9 at Sogndal.

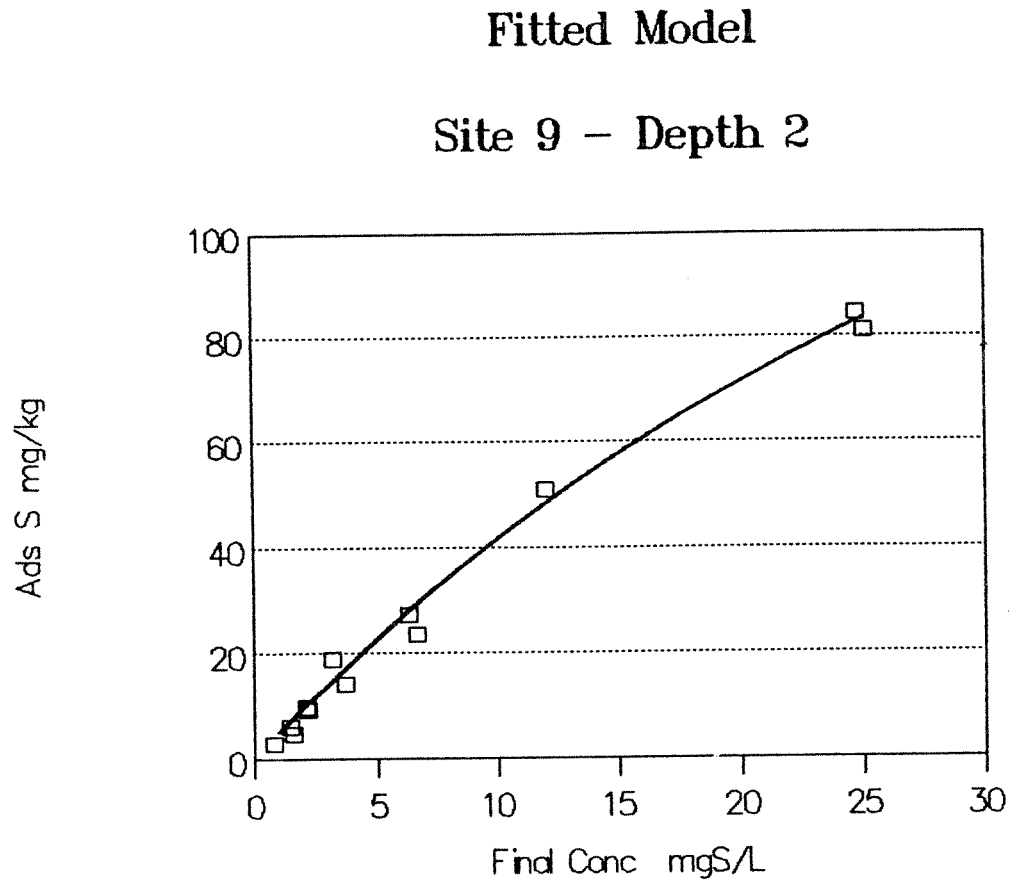


Figure 2.3. Langmuir isotherm for $SO_4^{2-}$ adsorption for the 15-30 cm depth at sampling site 9 at Sogndal as fit using the non-linear regression procedure.

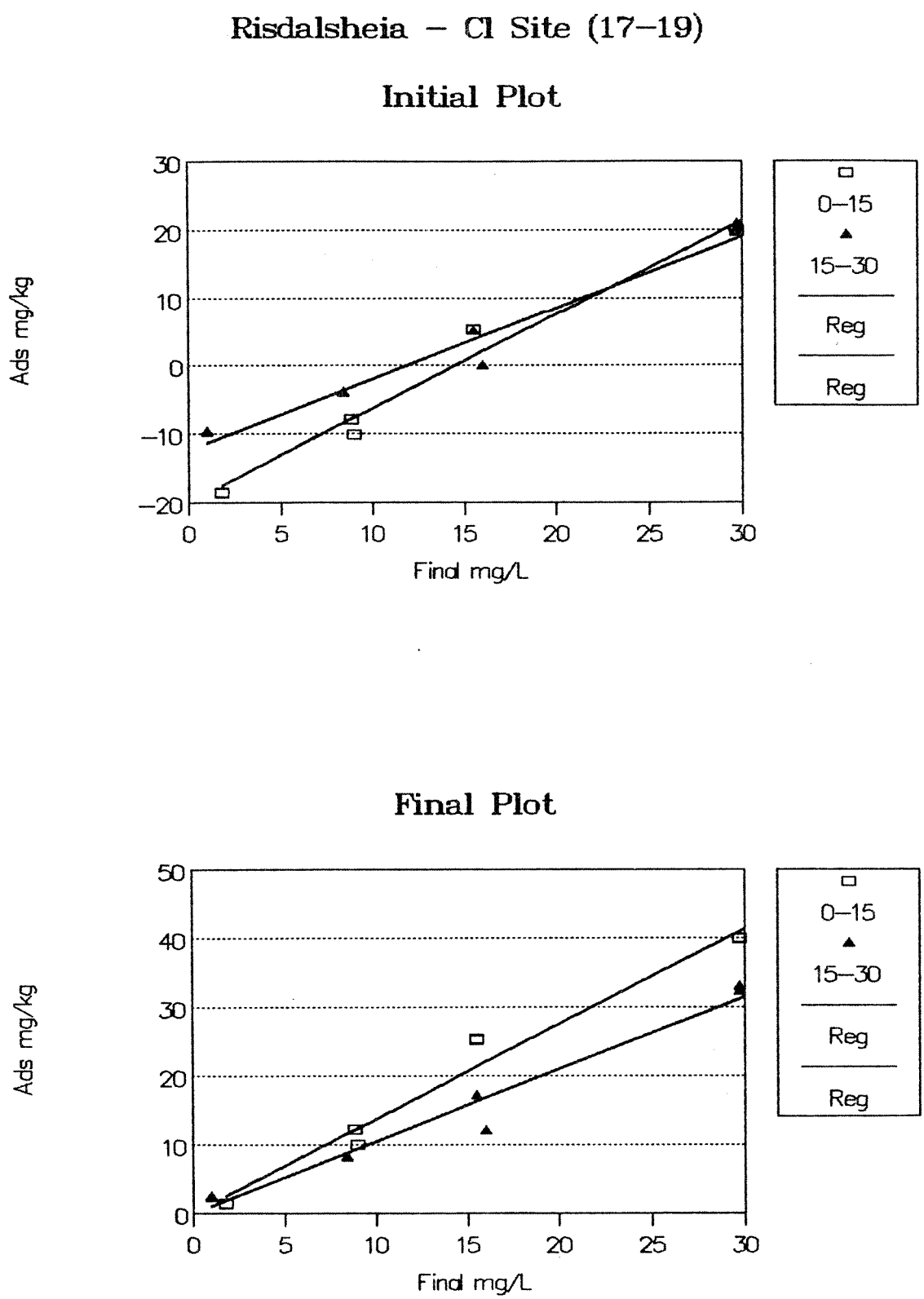


Figure 3.1. Initial uncorrected plot and final corrected plot for $Cl^-$ adsorption/desorption for sampling site (17-19) at Risdalsheia.

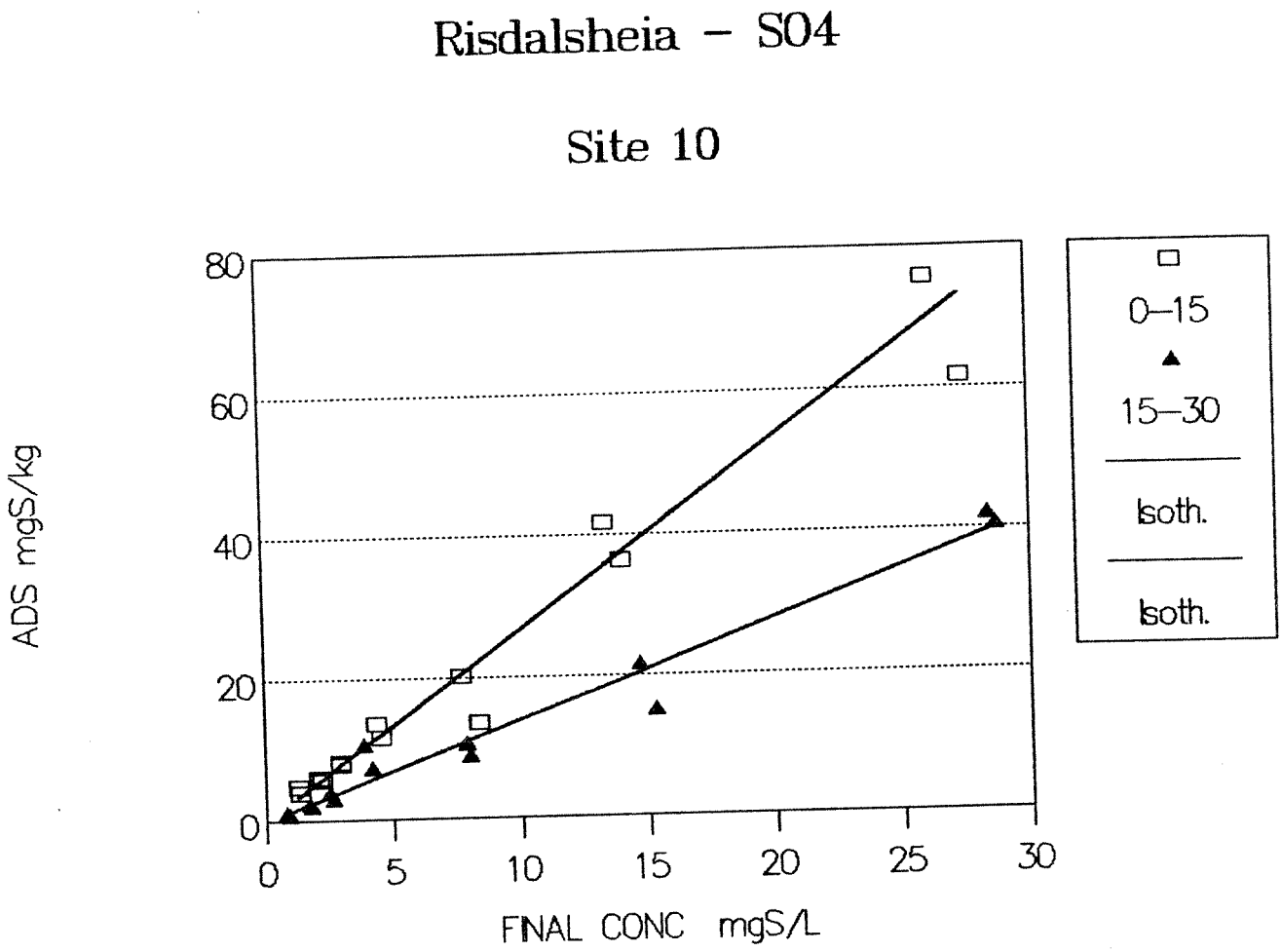


Figure 4.1. Final corrected $SO_4^{2-}$ adsorption for sampling site 10 at Risdalsheia. Only the linear isotherms were fitted in this case.

## APPENDICES

Table A 1. Risdalsheia, distribution parameters for cation exchange capacity (KCL) in meq/100 g.

| Depth | n | mean | Median | s.d. | Central Tendency[a] | NP Index[b] |
|---|---|---|---|---|---|---|
| Raw data | | | | | | |
| All | 115 | 9.97 | 9.43 | 6.04 | 9.97 | P |
| 0-15 | 46 | 14.94 | 13.74 | 5.82 | 14.94 | P |
| 15-30 | 46 | 7.17 | 7.11 | 3.18 | 7.17 | G |
| 30-45 | 23 | 5.64 | 5.39 | 3.37 | 5.64 | P |
| > 15 | 69 | 6.66 | 6.26 | 3.3 | 6.66 | P |
| Log (base e) Transform | | | | | | |
| All | 115 | 2.11 | 2.24 | 0.66 | 8.22 | F |
| 0-15 | 46 | 2.635 | 2.621 | 0.365 | 13.94 | F |
| 15-30 | 46 | 1.859 | 1.962 | 0.252 | 6.42 | F |
| 30-45 | 23 | 1.538 | 1.685 | 0.662 | 4.66 | F |
| > 15 | 69 | 1.752 | 1.834 | 0.576 | 5.77 | G |
| Square Root Transform | | | | | | |
| All | 115 | 3.017 | 3.071 | 0.937 | 9.1 | F |
| 0-15 | 46 | 3.8 | 3.707 | 0.717 | 14.44 | F |
| 15-30 | 46 | 2.608 | 2.667 | 0.611 | 6.8 | F |
| 30-45 | 23 | 2.27 | 2.322 | 0.721 | 5.15 | F |
| > 15 | 69 | 2.495 | 2.502 | 0.441 | 6.23 | G |

a. Central tendency is the population mean for the raw data, the geometric mean for the log transform, and the square of the square root mean for the square root transform.

b. The N P Index refers to a subjective evaluation of the linearity of the normal probability plots. Categories are Very Good, Good, Fair, and Poor.

Table A 2. Risdalsheia, distribution parameters for exchangeable Ca+Mg (meq/100g).

| Depth | n | mean | Median | s.d. | Central Tendency[a] | NP Index[b] |
|---|---|---|---|---|---|---|
| Raw data | | | | | | |
| All | 115 | 1.54 | 0.84 | 1.81 | 1.54 | VP |
| 0-15 | 46 | 2.96 | 2.31 | 2.01 | 2.96 | P |
| 15-30 | 46 | 0.65 | 0.38 | 0.78 | 0.65 | VP |
| 30-45 | 23 | 0.48 | 0.19 | 0.65 | 0.48 | VP |
| > 15 | 69 | 0.59 | 0.33 | 0.74 | 0.59 | VP |
| Log(base e) Transform | | | | | | |
| All | 115 | -0.39 | -0.174 | 1.48 | 0.68 | F |
| 0-15 | 46 | 0.871 | 0.839 | 0.67 | 2.39 | G |
| 15-30 | 46 | -1.06 | -0.968 | 1.18 | 0.35 | G |
| 30-45 | 23 | -1.57 | -1.66 | 1.4 | 0.21 | F |
| > 15 | 69 | -1.23 | -1.109 | 1.61 | 0.29 | G |
| Square Root Transform | | | | | | |
| All | 115 | 1.045 | 0.917 | 0.671 | 1.09 | VP |
| 0-15 | 46 | 1.632 | 1.52 | 0.551 | 2.66 | F |
| 15-30 | 46 | 0.695 | 0.616 | 0.412 | 0.48 | P |
| 30-45 | 23 | 0.574 | 0.436 | 0.402 | 0.33 | P |
| > 15 | 69 | 0.655 | 0.575 | 0.41 | 0.43 | P |

a. Central tendency is the population mean for the raw data, the geometric mean for the log transform, and the square of the square root mean for the square root transform.

b. The N P Index refers to a subjective evaluation of the linearity of the normal probability plots. Categories are Very Good, Good, Fair, and Poor.

Table A 3. Risdalsheia, distribution parameters for (Ca+Mg) saturation.

| Depth | n | mean | Median | s.d. | Central Tendency[a] | NP Index[b] |
|---|---|---|---|---|---|---|
| Raw data | | | | | | |
| All | 115 | 0.118 | 0.101 | 0.087 | 0.118 | VP |
| 0-15 | 46 | 0.18 | 0.193 | 0.073 | 0.18 | G |
| 15-30 | 46 | 0.076 | 0.056 | 0.064 | 0.076 | VP |
| 30-45 | 23 | 0.065 | 0.031 | 0.057 | 0.065 | VP |
| > 15 | 69 | 0.072 | 0.049 | 0.061 | 0.072 | VP |
| Log (base e) Transform | | | | | | |
| All | 115 | -2.496 | -2.287 | 0.937 | 0.082 | P |
| 0-15 | 46 | -1.766 | -1.644 | 0.435 | 0.171 | F |
| 15-30 | 46 | -2.92 | -2.883 | 0.859 | 0.054 | F |
| 30-45 | 23 | -3.106 | -3.488 | 0.881 | 0.049 | F |
| > 15 | 69 | -2.982 | -3.005 | 0.864 | 0.051 | F |
| Square Root Transform | | | | | | |
| All | 115 | 0.317 | 0.319 | 0.131 | 0.1 | P |
| 0-15 | 46 | 0.423 | 0.44 | 0.087 | 0.178 | G |
| 15-30 | 46 | 0.254 | 0.237 | 0.109 | 0.064 | VP |
| 30-45 | 23 | 0.232 | 0.175 | 0.105 | 0.054 | VP |
| > 15 | 69 | 0.247 | 0.222 | 0.107 | 0.061 | p |

a. Central tendency is the population mean for the raw data, the geometric mean for the log transform, and the square of the square root mean for the square root transform.

b. The N P Index refers to a subjective evaluation of the linearity of the normal probability plots. Categories are Very Good, Good, Fair, and Poor.

Table A 4. Risdalsheia, distribution parameters for K saturation.

| Depth | n | mean | Median | s.d. | Central Tendency[a] | NP Index[b] |
|---|---|---|---|---|---|---|
| Raw data | | | | | | |
| All | 114 | 0.021 | 0.021 | 0.0090 | 0.021 | P |
| 0-15 | 46 | 0.029 | 0.028 | 0.0062 | 0.028 | G |
| 15-30 | 46 | 0.017 | 0.017 | 0.0074 | 0.017 | F |
| 30-45 | 23 | 0.014 | 0.014 | 0.0058 | 0.014 | F |
| > 15 | 69 | 0.016 | 0.015 | 0.0067 | 0.016 | F |
| Log (base e) Transform | | | | | | |
| All | 114 | -3.954 | -3.871 | 0.473 | 0.019 | G |
| 0-15 | 46 | -3.572 | -3.564 | 0.211 | 0.028 | VG |
| 15-30 | 46 | -4.160 | -4.098 | 0.420 | 0.016 | G |
| 30-45 | 22 | -4.323 | -4.230 | 0.416 | 0.013 | G |
| > 15 | 68 | -4.213 | -4.177 | 0.423 | 0.015 | G |
| Square Root Transform | | | | | | |
| All | 114 | 0.142 | 0.144 | 0.0317 | 0.020 | F |
| 0-15 | 46 | 0.169 | 0.168 | 0.0180 | 0.028 | G |
| 15-30 | 46 | 0.128 | 0.129 | 0.0267 | 0.016 | G |
| 30-45 | 22 | 0.118 | 0.121 | 0.0239 | 0.014 | F |
| > 15 | 68 | 0.120 | 0.124 | 0.0261 | 0.016 | G |

a. Central tendency is the population mean for the raw data, the geometric mean for the log transform, and the square of the square root mean for the square root transform.

b. The N P Index refers to a subjective evaluation of the linearity of the normal probability plots. Categories are Very Good, Good, Fair, and Poor.

Table A 5. Risdalsheia, distribution parameters for density, (kg/l).

| Depth | n | mean | Median | s.d. | Central Tendency[a] | NP Index[b] |
|---|---|---|---|---|---|---|
| Raw data | | | | | | |
| All | 80 | 0.524 | 0.45 | 0.356 | 0.524 | P |
| 0-15 | 35 | 0.263 | 0.24 | 0.149 | 0.263 | F |
| 15-30 | 33 | 0.72 | 0.62 | 0.334 | 0.72 | G |
| 30-45 | 12 | 0.746 | 0.67 | 0.361 | 0.746 | G |
| > 15 | 45 | 0.727 | 0.62 | 0.338 | 0.727 | F |
| Log (base e) Transform | | | | | | |
| All | 80 | -0.9136 | -0.799 | 0.79 | 0.401 | P |
| 0-15 | 35 | -1.509 | -1.427 | 0.63 | 0.221 | G |
| 15-30 | 33 | -0.462 | -0.478 | 0.568 | 0.63 | F |
| 30-45 | 12 | -0.421 | -0.406 | 0.553 | 0.656 | F |
| > 15 | 45 | -0.451 | -0.478 | 0.558 | 0.637 | P |
| Square Root Transform | | | | | | |
| All | 80 | 0.681 | 0.671 | 0.248 | 0.464 | P |
| 0-15 | 35 | 0.493 | 0.49 | 0.147 | 0.243 | G |
| 15-30 | 33 | 0.823 | 0.787 | 0.21 | 0.677 | F |
| 30-45 | 12 | 0.838 | 0.817 | 0.218 | 0.702 | F |
| > 15 | 45 | 0.827 | 0.787 | 0.21 | 0.684 | F |

a. Central tendency is the population mean for the raw data, the geometric mean for the log transform, and the square of the square root mean for the square root transform.

b. The N P Index refers to a subjective evaluation of the linearity of the normal probability plots. Categories are Very Good, Good, Fair, and Poor.

Table A 6. Risdalsheia, distribution parameters for CEC (KCl) by volume (meq/l).

| Depth | n | mean | Median | s.d. | Central Tendency[a] | NP Index[b] |
|---|---|---|---|---|---|---|
| Raw data | | | | | | |
| All | 80 | 36.5 | 35.4 | 16.15 | 36.5 | P |
| 0-15 | 35 | 32.55 | 29.4 | 13.72 | 32.55 | P |
| 15-30 | 33 | 43.1 | 39.11 | 18.18 | 43.1 | G |
| 30-45 | 12 | 29.95 | 29.45 | 10.13 | 29.95 | G |
| > 15 | 45 | 39.58 | 36.48 | 17.33 | 39.58 | F |
| Log (base e) Transform | | | | | | |
| All | 80 | 3.499 | 3.569 | 0.453 | 33.08 | G |
| 0-15 | 35 | 3.392 | 3.381 | 0.44 | 29.72 | F |
| 15-30 | 33 | 3.669 | 3.666 | 0.455 | 39.21 | G |
| 30-45 | 12 | 3.345 | 3.379 | 0.35 | 28.36 | G |
| > 15 | 45 | 3.583 | 3.597 | 0.45 | 35.98 | VG |
| Square Root Transform | | | | | | |
| All | 80 | 5.898 | 5.957 | 1.319 | 34.79 | G |
| 0-15 | 35 | 5.579 | 5.423 | 1.208 | 31.12 | P |
| 15-30 | 33 | 6.417 | 6.254 | 1.401 | 41.18 | VG |
| 30-45 | 12 | 5.4 | 5.421 | 0.93 | 29.16 | G |
| > 15 | 45 | 6.146 | 6.04 | 1.361 | 37.77 | G |

a. Central tendency is the population mean for the raw data, the geometric mean for the log transform, and the square of the square root mean for the square root transform.

b. The N P Index refers to a subjective evaluation of the linearity of the normal probability plots. Categories are Very Good, Good, Fair, and Poor.

Norwegian Institute for Water Research NIVA

# Acid Rain Research Reports

**1/1982** Henriksen, A. 1982. Changes in base cation concentrations due to freshwater acidification. 50 pp. Out of print.

**2/1982** Henriksen, A. and Andersen, S. 1982. Forsuringssituasjonen i Oslomarkas vann. 45 pp. Out of print.

**3/1982** Henriksen, A. 1982. Preacidifcation pH-values in Norwegian rivers and lakes. 24 pp. Out of print.

**4/1983** Wright, R.F. 1983. Predicting acidification of North American lakes. 165 pp.

**5/1983** *Schoen, R.*, Wright, R.F. and *Krieter, M.* 1983. Regional survey of freshwater acidification in West Germany (FRG). 15 pp.

**6/1984** Wright, R.F. 1984. Changes in the chemistry of Lake Hovvatn, Norway, following liming and reacidification. 68 pp.

**7/1985** Wright, R.F. 1985. RAIN project. Annual report for 1984. 39 pp.

**8/1985** *Lotse, E.* and *Otabbong, E.* 1985. Physiochemical properties of soils at Risdalsheia and Sogndal: RAIN project. 48 pp.

**9/1986** Wright, R.F. and Gjessing, E. 1986. RAIN project. Annual report for 1985. 33 pp.

**10/1986** Wright, R.F., Gjessing, E., Semb, A. and Sletaune, B. 1986. RAIN project. Data report 1983-85. 62 pp.

**11/1986** Henriksen, A., Røgeberg, E.J.S., Andersen, S. and Veidel, A. 1986. MOBILLAB-NIVA, a complete station for monitoring water quality. 44 pp.

**12/1987** Røgeberg, E.J.S. 1987. A coulometric Gran titration method for the determination of strong and weak acids in freshwater. 28 pp.

**13/1987** Wright, R.F. 1987. RAIN project. Annual report for 1986. 90 pp.

**14/1988** Hauhs, M. 1988. Water and ion movment through a minicatchment at Risdalsheia, Norway. RAIN project. 74 pp.

**15/1988** Gjessing, E., Grande. M. and Røgeberg, E.J.S. 1988. Natural organic Acids. Their Role in Freshwater Acidification and Aluminium Speciation. 28 pp.

**16/1988** Wright, R.F. 1988. RAIN project. Annual report for 1987. 77 pp.

**17/1988** Wathne, B.M and Røgeberg, E.J.S. 1988. Buffering effects of river substrates under acidic conditions. 19 pp.

**18/1989** Lotse, E.G. 1989. Soil Chemistry 1983-86 at the RAIN Project Catchments. 66 pp.

**19/1989** Reuss, J.O. 1989. Interpretation of Soil Data from the RAIN Project. 81 pp.